JGR

Submitted to Journal of Geophysical Research

Modeling Modern Methane Emissions from Natural Wetlands 2. Interannual Variations 1982-1993

Bernadette P. Walter[1], Martin Heimann[2], and Elaine Matthews[1]

[1]Columbia University/NASA Goddard Institute for Space Studies, New York

[2]Max-Planck-Institut für Biogeochemie, Jena, Germany

Abstract. A global run of a process-based methane model [*Walter et al.*, this issue] is performed using high-frequency atmospheric forcing fields from ECMWF reanalyses of the period from 1982 to 1993. We calculate global annual methane emissions to be 260 Tg yr^{-1}. 25% of methane emissions originate from wetlands north of 30°N. Only 60% of the produced methane is emitted, while the rest is re-oxidized. A comparison of zonal integrals of simulated global wetland emissions and results obtained by an inverse modeling approach shows good agreement. In a test with data from two wetlands, the seasonality of simulated and observed methane emissions agrees well. The effects of sub-grid scale variations in model parameters and input data are examined. Modeled methane emissions show high regional, seasonal and interannual variability. Seasonal cycles of methane emissions are dominated by temperature in high latitude wetlands, and by changes in the water table in tropical wetlands. Sensitivity tests show that ±1 °C changes in temperature lead to ±20 % changes in methane emissions from wetlands. Uniform changes of ±20 % in precipitation alter methane emissions by about ±8 %. Limitations in the model are analyzed. Simulated interannual variations in methane emissions from wetlands are compared to observed atmospheric growth rate anomalies. Our model simulation results suggest that contributions from other sources than wetlands and/or the sinks are more important in the tropics than north of 30°N. In higher northern latitudes, it seems that a large part of the observed interannual variations can be explained by variations in wetland emissions. Our results also suggest that reduced wetland emissions played an important role in the observed negative methane growth rate anomaly in 1992.

1. Introduction

Starting in mid-1983 recent changes in the global atmospheric methane concentration have been monitored by the National Oceanic and Atmospheric Administration (NOAA) Climate Monitoring and Diagnostics Laboratory (CMDL). Atmospheric methane concentrations increased throughout the measurement period, but in the 1990s the growth rate slowed from ~14 ppbv yr^{-1} in 1984 to ~3 ppbv yr^{-1} in 1996 [*Dlugokencky et al.*, 1998]. Superimposed on this trend is considerable interannual variation. In 1992, for example, the global methane growth rate dropped dramatically and even became negative for a short period, but started to increase again in 1993. The causes for observed interannual variations and particular anomalies have not yet been fully identified. No comprehensive modeling study of the entire global methane cycle has been performed for that period, although variations in the OH sink, the wetland source [*Bekki and Law*, 1997] and the fossil fuel source [*Law and Nisbet*, 1996] have been studied. Numerous studies have been carried out in order to explain the strong negative growth rate anomaly in 1992 (section 3.3.1). It seems clear that no change in one single source (or sink), but a combination of changes in different sources and the sink was responsible for that anomaly. Until now, however, none of the proposed scenarios has been able to fully explain the atmospheric observations.

In pre-industrial times, wetlands constituted the dominant global methane source. However, since the beginning of the industrialization methane emissions from anthropogenic methane sources increased strongly. Table 1 lists global estimates for all major methane sources reported in two different studies [*Houweling et al.*, 1999; *Hein et al.*, 1997]. The estimate by *Hein et al.* is a "top-down" derived budget employing an inverse model; the authors used atmospheric methane measurements from the NOAA/CMDL network and some *a priori* information about the different methane sources and sinks. The uncertainties in the different source strengths were reduced by more than a third, but they are still considerable. *Houweling et al.* [1999] report a global methane budget that is based on "bottom-up" estimates, i.e., emission estimates for the different sources and (statistical) methods to extrapolate to the global scale. This budget was derived from various recent studies (Table 2 of *Houweling et al.* [1999]) and was used as an *a priori* estimate for their inverse modeling study (they did not distinguish between different methane sources in their *a posteriori* estimate). As the differences between these two estimates reveal, the uncertainties concerning the present global methane budget are still quite high. According to current estimates, natural wetlands constitute about 25-40% of the global methane source, and hence the largest single source at present. Many methane sources do not depend at all, or not very strongly, on climate, but methane emissions from wetlands are highly climate-sensitive because they are controlled by variations in soil temperature and soil moisture.

The aim of this study was to investigate the potential role of natural wetlands in the observed interannual variations of the atmospheric methane growth rate. A global climate-sensitive process based methane-hydrology model [*Walter et al.*, this issue] is used to study climate-induced changes in methane emissions from natural wetlands for the period from 1982-1993. The European Centre for Medium-Range Weather-Forecast (ECMWF) reanalyses [*Gibson et* *al.*, 1997] are used as forcing. The model is applied to the current global wetland distribution of *Matthews and Fung* [1987]. This is the first study to apply a global process-based model to simulate interannual variations in methane emissions from natural wetlands. *Cao et al.* [1996] calculated present-day global methane emissions from wetlands using a process-based model to simulate methane emissions based on the amount of decomposed organic carbon, water table and temperature. *Christensen et al.* [1996] used a process-oriented ecosystem source model to calculate present-day methane emissions from northern wetlands (>50°N) based on heterotrophic respiration. However, both models have not been applied to estimate interannual variations. *Bekki and Law* [1997] used a 2-dimensional chemistry-transport model and a simple temperature dependence for wetland emissions to calculate the effects of variations in wetland emissions on the methane growth rate for the period 1980-1992. However, only the effects of temperature, but not of changes in soil moisture on methane emissions were considered. Here we extend these modeling approaches by application of a process based model that takes the effects of both temperature and soil moisture into account to explore interannual variations.

Our global model results are compared to results obtained by the inverse modeling study of *Hein et al.* [1997] (section 3.1). A comparison with ground measurements is presented in section 3.2. In section 3.3 interannual variations of simulated methane emissions from wetlands are compared to interannual variations in the observed atmospheric methane growth rate. Finally, the sensitivities of simulated global methane emissions to changes in the climate input (soil temperature, precipitation and water table) and assumptions/parameterizations in the model are examined in section 3.4.

2. Model Forcing

The forcing for the global methane-hydrology model is shown in Figure 2 of *Walter et al.* [this issue]. This paper reports on model runs using European Centre for Medium-Range Weather Forecast (ECMWF) reanalyses [*Gibson et al.*, 1997] for the period 1982 to 1993 for the climate forcing. The forcing data are in T106 resolution (T106-truncation corresponds to 1.1° by 1.1°) and are linearly interpolated to a 1° by 1° grid. We use 24-hourly forecasts of total precipitation and soil temperature at several soil depths (levels 1-4) and 6-hourly forecasts of the 2m-(air) temperature, and surface solar and thermal radiation. 6-hourly forecasts are available 4 times a day and are used in cases where a diurnal cycle is needed. For precipitation, 24-hourly forecasts are used because they yield better results than forecasts over shorter periods [*Stendel and Arpe*, 1997]. Daily Net Primary Productivity (NPP) is obtained from monthly NPP values calculated by the global terrestrial carbon cycle model Biosphere-Energy

Transfer and Hydrology (BETHY) [*Knorr*, 1997]. The BETHY model is a process-based model describing the water balance on vegetated surfaces and bare soils and the CO_2 balance in vegetation and soils. It uses remote sensing data and calculates the NPP on a 0.5° by 0.5° grid with monthly time steps. The output of the BETHY model is linearly interpolated to daily values on a 1° by 1° grid.

3. Results and Discussion

3. 1. Global Methane Emissions from Wetlands

Figure 1 shows the average of the simulated annual mean methane fluxes from natural wetlands for 1982-1993. Annual mean fluxes range from a few mg m^{-2} d^{-1} to more than 400 mg m^{-2} d^{-1}. Per grid cell methane emissions in Gg yr^{-1} calculated using the actual wetland areas of each wetland grid-cell are plotted in Figure 2a. Simulated annual mean fluxes are usually larger in lower latitudes owing to differences in active season lengths which are longer in low latitudes; also, they are usually larger in regions where annual total fractional oxidation (the percentage of produced methane that is re-oxidized in soil; Figure 2b) is lower. In the only other global modeling study of methane emissions from wetlands, *Cao et al.* [1996] find a similar spatial pattern of annual methane emissions from wetlands; however, their global wetland source strength is 92 Tg yr^{-1} and hence considerably lower than in this study (section 3.1.1). In the methane model, globally and annually, only about 60% of the produced methane is emitted, the rest is re-oxidized in soil. Annual total fractional oxidation is the sum of annual soil oxidation (Figure 2c) and annual rhizospheric oxidation (Figure 2d). Figure 2a helps to convert fractional oxidation (%) into amounts of methane. As discussed in *Bogner et al.* [2000] in the methane model, soil oxidation is controlled by the position of the water table, and rhizospheric oxidation by vegetation. If the water table is below the soil surface, methane is partly oxidized in the oxic top soil. In northern high latitude wetlands, for example, annual soil oxidation is larger in regions where the water table is lower during the active season (compare Figure 9 of *Walter et al.* [this issue] and Figure 2c). Part of the methane transported through plants is oxidized in the rhizosphere (see sections 2 and 3.3 of *Walter et al.* [this issue]), increasing rhizospheric oxidation and hence total fractional oxidation. If the water table is below the soil surface, however, methane transported through plants bypasses the oxic top soil, leading to decreased soil oxidation and hence reduced total fractional oxidation. Therefore, regions where rhizospheric oxidation is large can still be regions where methane fluxes are large, since the fraction of methane emitted through plants is also large.

Zonally integrated annual methane emissions over the period 1982-1993 are shown in Figure 3a. The comparison with the results of an inverse modeling study by *Hein et al.* [1997] (Figure

3b) shows that both methods have a peak around the equator and another peak around 60°N. A comparison with the zonally-integrated wetland areas of *Matthews and Fung* [1987] (Figure 3c) shows that these two peaks are related to peaks in wetland areas. As discussed in section 3.1.1, *Hein et al.* [1997] give a slightly lower value for global annual methane emissions from wetlands, and the peak around the equator is less pronounced in their study than in ours. In both studies, however, about 25% of the global annual emissions originates from higher northern latitude (>30°N) wetlands (which constitute 60% of the global wetland area). Given the differences in methods between these two studies the similarity between the results suggests that they are robust.

3. 1. 1. Global Wetland Source Strength

The 1983-1992 mean of simulated methane emissions is 260 Tg yr^{-1}. This value is at the high end of current estimates of the global wetland source strength. The amplitude of simulated methane emissions depends on a factor, R_0, in the methane production rate; global values of R_0 are parameterized as a function of NPP and the annual mean temperature derived from 6 test sites where measurements of methane fluxes over at least one season were available [*Walter et al.*, this issue]. Compared to other studies [*Bartlett and Harris*, 1993; *Matthews*, 2000; and references therein] annual methane emissions from all test sites seem quite high which can explain the high global emission; a comparison with data from a Swedish mire and a Minnesota peatland presented in section 3.2 supports this hypothesis. A sensitivity test of the 1-dimensional methane model, however, has shown that changes in R_0 only change the amplitude of simulated methane emissions, but not the temporal emission pattern.

"Bottom-up" approaches use flux measurements and information on emission periods and wetland areas to extrapolate to global and annual scales; estimated global methane emissions range from 80 to 156 Tg yr^{-1} [*Aselmann and Crutzen*, 1989; *Matthews and Fung*, 1987; *Bartlett and Harriss*, 1993; *Lelieveld et al.*, 1998; *Khalil and Rasmussen*, 1983]. Even though seasonal and interannual variations in methane emissions are known to be high, only a few of the flux data sets used are of high frequency and cover periods of a season or more. In addition, fluxes are usually grouped based on wetland and/or vegetation type; the main factors controlling methane emissions, however, are water table, temperature and substrate quality [*Conrad*, 1989]. Wetland and vegetation types are certainly related to these factors, e.g., vegetation affects substrate quality. However, these factors and methane fluxes can vary widely within one wetland or vegetation type. Micrometeorological measurements, for example, that cover larger spatial scales [*Clement et al.*, 1995] or a climate-sensitive model using as many measurements as possible to extrapolate to the global scale could improve "bottom-up" approaches.

In a "top-down" approach *Hein et al.* [1997] used an inverse model to test different scenarios; they obtained a global wetland source strength of about 230 Tg yr^{-1} (±10%) if an *a priori* estimate of 270 Tg yr^{-1} was used, and of 200 Tg yr^{-1} (±10%) if an *a priori* estimate of 135 Tg yr^{-1} was used; i.e., a relatively large wetland source is obtained independent of the *a priori* source estimate. The major limitations of inverse modeling lie in the models used, the assumptions made and the sparse distribution of atmospheric data. As all "bottom-up" estimates agree that global wetland emissions are below 156 Tg yr^{-1} there is an apparent discrepancy which has not yet been resolved. Another method to constrain the current wetland source strength is to use an estimate of the pre-industrial wetland source. *Houweling* [1999] simulated pre-industrial methane employing a three-dimensional chemistry-transport model using methane mixing ratios and $\delta^{13}CH_4$ from ice cores as constraints; he tested different scenarios of pre-industrial sources and sinks and obtained a pre-industrial wetland source strength of 130-194 Tg yr^{-1}; he points out that cultivation and drainage could have reduced the pre-industrial wetland source by 10% (see references in *Houweling* [1999]). However, climatic changes since the beginning of industrialization could have increased global methane fluxes, as global mean temperatures have increased by about 0.7° since the late 1880s [*Hansen et al.*, 1999]; this climate-induced increase in global methane fluxes could even be larger than 10% (section 3.4.1).

In summary, global estimates for the wetland source strength vary between 80 and 230 Tg yr^{-1}. In this study a high value of 260 Tg yr^{-1} is obtained primarily, because the data sets (from the 6 test sites of the methane model, section 2 of *Walter et al.* [this issue]) used in the global extrapolation of the model show relatively high emissions. Overestimation of the global total should not compromise the capability of the model to investigate climate-induced spatial and temporal patterns which is the purpose of this study. However, a model like ours could be used to improve "bottom-up" estimates, if a different global extrapolation based on as many data as possible is used.

3. 2. Comparison with Ground Measurements

The 1-dimensional methane model was successfully tested at 6 sites, where time-series of the input and output data of the methane model and information on model parameters were available [*Walter and Heimann*, 2000]. For a test of the global methane-hydrology model data representative of larger spatial scales are needed. Global measurements of atmospheric methane concentrations are one possibility (section 3.3). Regional estimates of annual methane emissions exist in a few places [*Reeburgh et al.*, 1998; *Roulet et al.*, 1994; *Tathy et al.* 1991; *Devol et al.*, 1990; *Bartlett et al.*, 1988]. However, they are far too sparse, to test if the spatial pattern of modeled methane emissions is realistic. Time-series of methane emissions on spatial scales comparable to the model's 1^o by 1^o grid are not available. Therefore, we use two data sets consisting of time-series of methane flux measurements that are representative of a whole wetland, i.e., of an area of about 1 by 1 km^2. At both sites chamber measurements were made in different parts of the wetland and at one site also eddy correlation measurements were performed.

Svensson et al. [1999] report methane measurements made in a subarctic Swedish mire (Stordalen mire, 68°N, 21°E) in 1974, 1994 and 1995. They measured methane fluxes in dry and wet, and in ombrotrophic (nutrient deficient) and minerotrophic (nutrient rich) parts of the wetland. Fluxes from the dry parts were very low. In the wet parts fluxes from minerotrophic soils were considerably higher than from ombrotrophic soils (Figure 4). These differences are attributable to differences in soil chemistry and vegetation, since water tables and temperatures were similar at all wet sites. They show how large sub-grid scale variations can be. Modeled fluxes from the grid-cell where the wetland is located and the next surrounding grid-cells were compared to the data. Fluxes from surrounding grid-cells were included in order to avoid that the effect of one particular R_0 value or another model parameter becomes dominant. As no modeling results are available for any of the years of observation the mean (±1 standard deviation) of modeled methane emissions from all considered grid-cells and years (1982-1993) is compared to the data (Figure 4). Since observed fluxes from all 3 years were similar this should not limit the comparison. Figure 4 shows that the seasonal cycle of observed methane fluxes is well captured by the model. The magnitude of the model results is comparable to the magnitude of emissions from minerotrophic soils which suggests that the 6 test sites used to calibrate the model, i.e., to derive R_0 (*Walter at al.* [this issue] and section 3.1.1) were sites with high substrate quality favoring high emissions. Hence, R_0 is not necessarily overestimated, but different R_0 values should be used within a grid-cell to account for varying substrate quality. Global data sets to derive wetland fractions of different peat quality are still lacking. Therefore, with the current model sub-grid scale variations in model parameters such as R_0 cannot be considered. However, this needs to be improved in the future.

The data set of *Clement et al.* [1995] consists of eddy correlation and chamber measurements from a peatland in central Minnesota (Bog Lake peatland, 48°N, 93°W) made during 1991-1992. The chamber measurements were made from different hummock/hollow pair locations. The seasonal patterns of fluxes obtained by the two techniques compared well, however, the magnitudes were slightly different. Up-scaling of the chamber measurements using information on microtopography reduced this discrepancy. Figure 5 shows a comparison between simulated and observed methane fluxes (1. row; as above simulated methane emissions from the grid-cell, where the wetland is located, and the surrounding grid-cells are used) and water table (2. row, the observed water table is depicted relative to the average hollow surface which is about 35 cm lower than the average hummock surface); in rows 3 and 4 model input, i.e., ECMWF precipitation and temperature are compared to observations made at the wetland site. ECMWF temperature and observed temperature are very similar. ECMWF precipitation is slightly higher than observations in 1991, but the patterns are similar. In 1992, however, ECMWF precipitation is generally lower than observations and they differ considerably in June when observed precipitation is twice as high as ECMWF precipitation. This is an example of how large sub-grid scale variations in precipitation can be. However, re-analysis precipitation is not always realistic [*Stendel and Arpe*, 1997]. These differences in the input data affect simulated water tables. In 1991 simulated and observed water table compare well. In 1992 simulated and observed water table are similar until June when the observed water table rises to the soil surface due to extremely high precipitation in June. As ECMWF precipitation is much lower, the simulated water table remains below the soil surface. These differences in water table affect modeled methane fluxes. In 1991 the seasonal pattern of simulated and observed methane emissions agree well, the magnitude of simulated methane emissions, however, is bigger than in the observations. This implies that the R_0 values used in the model are very high, and that differences in substrate quality affecting R_0 need to be included in the future. Since in 1992 the simulated water table is below the soil surface during the most productive time (June-August) simulated emissions are considerably lower than in 1991. This big drop in methane emissions is not seen in the observations, because the observed water table is above the soil surface during June-August of 1992. Slightly lower temperatures in 1992 also contribute to that drop in emissions, and observed methane fluxes are also slightly lower in 1992 than in 1991. However, the main difference between observations and model results in 1992 is due to differences in the input data. Hence, sub-grid scale variations and/or limitations in the input data (mainly precipitation) can have a strong effect on modeling results.

In summary, at both test sites the seasonality of simulated and observed methane emissions agreed well. However, the results suggest that R_0 in the model is very high, and that different R_0 values should be used within one grid-cell to account for variations in substrate quality. In addition, sub-grid scale variations in the input data (mainly precipitation) and/or limitations in the used input data can also affect modeling results.

3. 3. Interannual Variations during 1982-1993

Figure 6 shows the zonally integrated simulated methane emissions for the period 1982-1993. Simulated methane emissions show considerable seasonal and interannual variations. In higher northern latitudes simulated methane emissions show a pronounced seasonal cycle with high emissions in the summer and no or very low emissions in the winter. In higher latitude wetlands the seasonal cycle of simulated methane emissions is mainly controlled by the seasonal cycle of soil temperature; in low latitude wetlands where temperature does not change much during the year, the seasonal cycle of simulated methane emissions is dominated by the seasonal cycle of the water table. In northern low latitude wetlands there is a dry season between February and May, in southern low latitude wetlands between August and November (see Figure 9 in *Walter et al.* [this issue]). During the dry season, the water table drops so much below the soil surface that the wetland is practically dry and methane emissions become zero. Peak methane emissions are similar in low and high latitude wetlands. Simulated methane fluxes vary interannually; for example, a pronounced negative emission anomaly occurs in higher norther latitudes in 1992 (section 3.3.1).

Interannual variations in simulated methane emissions and their causes are further investigated, and they are compared to atmospheric observations (Figure 7). The left column of Figure 7 shows global results, the right column shows results for the higher northern hemisphere (HNH, >30°N). The first two rows (Figures 7a-d) show comparisons between model results and atmospheric observations [*Dlugokencky et al.*, 1998] which started in mid-1983. The model results in Figures 7a-d are always simulated methane emission anomalies from natural wetlands. The global observations (Figures 7a and c) are observed atmospheric methane growth rate anomalies. The "observed" anomalous methane source shown in Figures 7b and d, 10, 11, and 13 was inferred from the seasonally corrected and zonally averaged atmospheric CH_4 concentration measurements [*Dlugokencky et al.*, 1998] by means of an inversion procedure using a simple 3-box meridional mixing model of the atmosphere divided at 30°N and 30°S. Thereby the mixing parameters of the 3-box model were determined from atmospheric measurements of Sulfurhexafluoride (SF_6) [*Levin and Hessheimer*, 1996]. The first row shows filtered (cutoff frequency: (15 month)$^{-1}$, pass-through frequency: (36 month)$^{-1}$) monthly values and the second row annual totals. In all cases observed atmospheric methane growth rates were detrended, assuming that the observed trend in the atmospheric methane growth rate is caused by changes in other methane sources and the sinks. Recent studies indicate that global OH concentrations increased over the last 2 decades and that methane emissions are still increasing [*Kroll et al.*, 1998; *Karlsdottir and Isaksen*, 2000]; for example, fossil fuel emissions [*Law and Nisbet*, 1996], methane emissions from biomass burning [*Hao* *and Ward*, 1993], and rice paddy emissions [*Shearer and Khalil*, 1993; *Denier van der Gon*, 2000] have increased in the last decades; estimates of methane emissions from animals and landfills also show an increase over this period [*Matthews et al.*, 1998]. Our results reveal that over the 12 year simulation period there is no trend in methane emissions from wetlands. The comparisons between model results and atmospheric observations show that the anomalies in the data and the model results are in the same order of magnitude, the simulated anomalies being slightly higher. This could be, in part, because, as discussed in section 3.1.1, total simulated methane emissions seem to be overestimated. In a modeling study using a 2-dimensional chemistry-transport model and a simple temperature dependence for wetland emissions, *Bekki and Law* [1997] calculated the effect of variations in wetland emissions on the methane growth rate for the period from 1980-1992. As they used a lower temperature sensitivity and smaller wetland source than in our study, the magnitude of their results is smaller. However, in years when water table variations are small, the patterns in their and our results are comparable.

In several years, there is good agreement between model results and observations, particularly in the annual anomalies (Figures 7c and d). In general, the agreement between model results and observations is better in the HNH than globally; in the HNH from 1988-1993, model results and observations show a similar phase behavior. Therefore, our results suggest that, particularly in the HNH, observed anomalies in the atmospheric methane growth rate are, to a large extent, explained by methane emission anomalies from natural wetlands. Discrepancies between model results and observations in Figures 7a-d are either due to contributions from other sources and/or the sinks, and/or due to shortcomings in the model. A detailed discussion of the possible causes for discrepancies between model results and observations in Figures 7a-d is presented in section 3.5.

Factorial experiments were carried out to investigate and separate the impacts of anomalies in soil temperature and in water table on simulated methane emission anomalies (Figure 7e and f). Anomalies caused by soil temperature variations are calculated using the "mean" seasonal cycle of the water table (the mean of the 1982-1993 period), but the original soil temperature as input files for the methane model. The same approach was used for water table anomalies. In some years, the effects of soil-temperature and water-table anomalies on emission anomalies are of similar magnitude, but different in sign (e.g., in 1982, 1984, 1988, and 1993 in Figure 7e, and in 1982, 1988 and 1993 in Figure 7f). In these years, these offsets result in small simulated anomalies. In contrast, large emission anomalies occur in years when the effect of either soil temperature or water table dominates, or when both operate to either increase or reduce emissions. In the HNH, 50% of emission variations are caused by temperature and 50% by water table variations; globally temperature variations are responsible for about 60% of simulated variations. These results confirm that precipitation anomalies strongly influence our modeling results; hence inclusion of precipitation is important for modeling methane emission anomalies from wetlands.

Figures 7g and h show anomalies (%, relative to the respective maximum anomalies of the period 1982-1993) in soil temperature and precipitation, which are input data of the global methane-hydrology model (see Figure 2 of *Walter et al.* [this issue]). Figure 7g shows annual temperature and precipitation anomalies, Figure 7h anomalies for May-October, which is approximately the period of the productive season in the HNH (see Figure 6). The response of the methane model to changes in temperature is almost instantaneous if the water table remains unchanged [*Walter et al.*, 1996; *Walter and Heimann*, 2000]. The response of the hydrologic model to changes in precipitation is more complex, since water is stored in soil. However more precipitation generally leads to higher water tables (see Figures 7 and 8 of *Walter et al.* [this issue]). So, in almost all cases temperature and precipitation anomalies, respectively, translate into temperature-dependent and water table-dependent emission anomalies of the same sign (compare Figure 7, rows 3 and 4). The reasons for differences between input data anomalies and the results in the factorial experiments are: (1) the synchronicity of the anomalies in temperature and precipitation can affect results: for example, temperature anomalies translate into emission anomalies only during the productive season; (2) if a negative precipitation anomaly is large and causes a large negative water-table anomaly, a coincident temperature anomaly does not strongly impact methane emission (for example, Figure 7g; 1987 and 1989).

3. 3. 1. The 1992 Anomaly

Figure 8 (top, left) shows a global map of simulated annual methane-emission anomalies (%) for 1992 relative to the 1982-1993 mean. Figure 8 (top, right) shows May-October temperature (^{o}C) and precipitation (%) anomalies for 1992 relative to the 1982-1993 mean for the HNH only; in Figure 8, bottom, annual precipitation (%) and temperature (^{o}C) anomalies for 1992 relative to the 1982-1993 mean are plotted. In 1992, productive season (May-October) temperature anomalies are negative almost throughout all HNH wetlands and simulated methane emission anomalies are negative in most of the HNH wetlands. Those regions in the HNH, however, where simulated methane emission anomalies are positive are regions where May-October precipitation anomalies are positive (Alaska, Hudson Bay, parts of Siberia). In the tropics temperature anomalies are generally small in 1992 and simulated methane emission anomalies occur in regions with precipitation anomalies. Therefore, the large simulated negative methane emission anomaly in the HNH in 1992 is caused by the large negative temperature anomaly after the eruption of Mt. Pinatubo that coincides with a large negative precipitation (and hence water table) anomaly (see also Figure 7f); i.e., the large extent of this anomaly is caused by the coincidence of large negative temperature and precipitation anomalies and cannot be explained by temperature variations alone. The methane model, however, overestimates the magnitude (Figure 7d) in the HNH. This could be explained by (1) the fact that the methane model overestimates total annual global methane emissions as discussed in section 3.1; by (2) the fact that the effect of microtopography on sub-grid scale hydrology is not considered in the model (section 3.4.2, Figure 10); or (3) by an increase in (an)other HNH source(s) or a decrease in the HNH sink.

In the HNH, the 1992 anomaly is the largest in the model results and in the data. Therefore, our model results strongly suggest that reduced methane emissions from HNH wetlands largely contributed to that anomaly. A large contribution of northern wetlands was proposed earlier by *Hogan and Harris* [1994].

After the eruption of Mt. Pinatubo, decreased tropospheric temperatures were observed [*Dutton and Christy*, 1992] along with increased stratospheric temperatures [*Labitzke*, 1994], and decreased stratospheric O_3 [*Gleason et al.*, 1993]. Based on these observations, *Bekki et al.* [1994] proposed that increased atmospheric OH concentrations caused by stratospheric O_3 depletion could partly explain the 1992 anomaly; *Schauffler and Daniel* [1994] suggested the subsidence of stratospheric air masses because of increased stratospheric circulation caused by increased stratospheric temperature. Both scenarios would cause a decreased methane growth rate and a positive $\delta^{13}C$ anomaly. Since wetlands are isotopically light (-67 to -53‰, the global mean $\delta^{13}C$ is -47‰ [*Quay et al.*, 1991; and references therein]), a reduction in the wetland source alone would also cause a positive $\delta^{13}C$ anomaly.

Based on data showing a negative $\delta^{13}C$ anomaly, *Lowe et al.* [1997] suggest a large reduction (of about 20 Tg yr^{-1}) in a very heavy source (biomass burning (-32 to -24‰ [*Quay et al.*, 1991; and references therein]); *Gupta et al.* [1996] propose a combination of increased emissions from light sources (rice paddies, animals, and landfills) and decreased emissions from heavy sources (biomass burning, fossil fuel). *Dlugokencky et al.* [1994] suggested also reduced fossil fuel emissions from the FSU as a cause for the 1992 anomaly. However, until now the global and temporal coverage of isotopic measurements is sparse and data sets of atmospheric methane isotopes do not agree particularly for the early 1990s and 1992 [e.g. *Francey et al.*, 1999]. *Lowe et al.* [1994] and *Tyler et al.* [1993] find a negative $\delta^{13}C$ anomaly, while *Etheridge* *et al.* [1998] report only a "short stabilization"; *Quay et al.* [1999] do not find a negative $\delta^{13}C$ anomaly in 1992 at all. Therefore, isotopic data do not currently seem to constitute a strong constraint on proposed scenarios and further work is necessary to resolve that discrepancy.

Furthermore, as proposed scenarios must be consistent with atmospheric data, it is necessary to justify suggested changes in sources; for example, not much is known about methane emissions from biomass burning and its interannual variations; indications for a decreased global biomass burning source in 1992 are sparse and restricted to very few regions (e.g., Amazon region [*Artaxo et al.*, 1994], Kruger National Park (W. Trollop in *Rudolph* [1994]). Increased emissions from rice paddies, animals and landfills as proposed in *Gupta et al.* [1996] were only very small in 1992 [*Matthews et al.*, 2000]. In addition, as stated by *Bekki and Law* [1997], proposed scenarios should be tested against the entire atmospheric methane record. The increase in methane growth rate after 1992, for example, makes a large reduction of gas leaks in the FSU, as suggested by *Dlugokencky et al.* [1994], unlikely. In the future, using a 3-dimensional model as proposed in section 3.5 could improve our understanding of the causes of the 1992 anomaly. However, this study emphasizes the influence of HNH wetlands to the 1992 anomaly.

3. 4. Sensitivity Tests

3. 4. 1. Sensitivity to Climate Input

Figure 9 shows results of sensitivity tests of the global methane model to changes in soil temperature (Figures 9 a,b) and water table (Figures 9 e,f), and of the global methane-hydrology model to changes in precipitation (Figures 9 c,d). The sensitivity tests were performed for one year (1988). Table 2 summarizes the changes in simulated annual global methane emissions (%) due to changes made in the input data.

The sensitivity of the global methane model to $\pm 1^{\circ}C$ changes in surface temperature was tested. For that purpose, the soil temperature of the upper soil (until 20 cm soil depth) was uniformly changed by $\pm 1^{\circ}C$. In order to be more realistic, the change is linearly decreased from $1^{\circ}C$ to $0.75^{\circ}C$ between 20-60 cm soil depth, and from $0.75^{\circ}C$ to $0.5^{\circ}C$ between 60-150 cm soil depth. Methane production and oxidation are the major temperature dependent processes in the methane model; the temperature dependence of production being much stronger (Q_{10}=6) than that of oxidation (Q_{10}=2). A $1^{\circ}C$ increase in temperature increases simulated global annual methane emissions by 20%, a $1^{\circ}C$ decrease in temperature reduces simulated global annual methane emissions by 17% (Table 2). Figures 9 a,b show that these changes in simulated annual methane emissions are generally independent of the latitude and hence the environmental conditions. These results agree well with results of sensitivity tests performed with the 1-dimensional methane model at different sites representing a variety of environmental conditions [*Walter and Heimann*, 2000]. At all sites $\pm 1^{\circ}C$ changes in temperature resulted in about ±20% changes in simulated methane emissions. This is a stronger response than obtained by *Cao et al.* [1998] and earlier studies using regression models [*Öquist and Svensson*, 1996], however, field observations showed an up to four-to five-fold increase in methane emissions if temperature increased by $4^{\circ}C$ [*Öquist and Svensson*, 1996]. These results give an idea of how big changes in methane emissions from natural wetlands can be under a changed climate. In order to make a more realistic estimate of the increase in methane emissions from natural wetlands owing to a possible global warming, however, one needs to use GCM output from a global change scenario experiment as input for the methane-hydrology model.

In the global methane-hydrology model, uniform changes in precipitation of +20%/-20% lead to changes in simulated global annual methane emissions of +8%/-9%, respectively (see Table 2 and Figures 9 c,d). 20% changes in precipitation have a much larger effect in higher latitudes; sensitivity tests with the hydrology model show that 20% changes in precipitation have a stronger effect on the seasonal cycle of the simulated water table in the HNH (see Figure 5 in *Walter et al.*, [this issue]). In the tropics during the dry season, precipitation is very low and therefore a 20% change does not have a large effect; during the wet season precipitation is extremely high causing standing water, and a change in precipitation of 20% changes run-off, but not the water table, in the hydrologic model. As discussed in *Walter et al.* [this issue], the parameterization of lateral inflow, L, in the hydrologic model leads to the problem that in some low latitude wetlands, the water table is slightly higher in years with lower precipitation, and vice versa ($20^{\circ}S$ and $20^{\circ}N$). This sensitivity test provides a range for possible variations in methane emissions from natural wetlands if precipitation changes under a changed climate.

In the global methane model, uniform changes in the water table of +10 cm/-10 cm change simulated global annual methane emissions by +17%/-27%, respectively. As with precipitation, the effect of a changed water table is, in general, larger at higher latitudes. In the methane model, simulated methane emissions are not affected by the depth of standing water; only changes in the water table below the soil surface affect simulated methane emissions. In the hydrologic model, owing to run-off, standing water rarely exceeds a depth of 10 cm (see Figure 5 in *Walter et al.* [this issue]). For that reasons, lowering the water table by 10 cm has a larger effect on simulated global annual methane emissions than raising it by 10 cm. Particulary at higher latitudes, the water table is often below the soil surface during the productive season; there lowering the water table by 10 cm means increasing the oxic top soil by 10 cm. At 10^oS simulated methane emissions are slightly smaller than in the control run if the water table is changed by +10 cm. Sensitivity tests with the 1-dimensional model have shown that this can happened in only one situation [*Walter*, 1998]; if the water table falls below the soil surface during the productive season when top soil methane concentrations are high, there is initially a peak in diffusive methane flux. This peak can be so high that for a short time (a few days) simulated fluxes are higher if the water table falls below the soil surface than if it stays above the soil surface. These results show that the response of the methane model to a changed water table is quite non-linear. Therefore, the correct calculation of the water table is crucial for simulating methane emissions from wetlands. The further development of the hydrologic model or a model that can even account for sub-grid scale variations in the water table is thus a priority for improving global modeling of emissions from natural wetlands

3. 4. 2. Sensitivity to Assumptions in the Global Methane-Hydrology Model

The following four assumptions/parameterizations that are made in the global methane-hydrology model are tested: (1) Only one "mean" water table is used for a grid cell; i.e., sub-grid scale variations in wetland elevation and hence hydrology are neglected; (2) the Q_{10} factor used to describe the temperature dependency of processes leading to methane production (which are production of substrate for methanogenesis and methane production itself) is globally set to 6; (3) globally a maximum methane oxidation rate of 20 $\mu M\ h^{-1}$ is used; (4) the effect of the parameterization of the lateral inflow, L, in the hydrologic model on simulated interannual variations in methane emissions from tropical wetlands is assessed.

(1) Usually a wetland has a certain microtopography with holes (hollows) and areas that are elevated several tens of centimeters relative to the overall wetland surface (hummocks). As a consequence the position of the water table relative to the soil surface is not the same throughout the wetland. A difference in the water table of a few tens of centimeters, however, can change methane emissions considerably. Since the water table calculated by the hydrologic model is considered to be the mean water table of the wetland, certain parts of the wetland have a higher water table, others have a lower water table. The following sensitivity test ("micro") is carried out to test how a more realistic treatment of the water table affects the modeling results. It is assumed that in 60% of the wetland area of each grid-cell the water table is the mean water table as calculated by the hydrologic model, 10% are hollows which are water-filled throughout the year, and the remaining 30% are hummocks or areas that are elevated so much relative to the overall wetland surface that methane emissions are zero. Figure 10 shows the results of the "micro" sensitivity test for the HNH (it is not expected that

microtopography has a large effect in the tropics, because during the wet season there is usually standing water). As in Figure 7b simulated interannual methane emission anomalies from wetlands are compared to observed atmospheric methane growth rate anomalies. Figure 10 shows that the "micro" assumption leads to smaller amplitudes in the model results. As methane emission anomalies seem to be overestimated in the control run, the amplitudes in the "micro" run are more comparable to amplitudes in the observations. Particulary in 1992 the "micro" run gives a better result. However, at times when model results (in the control run) and observations are out of phase, the "micro" assumption does not improve this. Therefore, considering sub-grid scale micrc topography can improve the results. In order to take sub-grid scale microtopography into account a hydrologic model to calculate the spatial (and temporal) variation of the water table within a 1^o by 1^o grid cell using a high resolution global topographic data set as, for example, in the TOPMODEL approach [*Stieglitz et al.*, 1997] will need to be developed.

(2) Observed Q_{10} values for the processes leading to methane production (production of substrate for methanogenesis and methane production itself) lie in the range from 1.7 to 16 [*Dunfield et al.*, 1993; *Valentine et al.*, 1994; *Westermann*, 1993]. Particulary in tropical rice paddies a low temperature dependence (Q_{10} in the order of 2) of methane production has been observed (H.-U. Neue, personal communication, 1998). Therefore, a sensitivity run using globally a Q_{10} of 2 (instead of 6) is carried out. We do not expect that a Q_{10} of 2 will improve the results in the HNH; in all tests of the model in HNH wetlands (using Q_{10}=6) the amplitudes of simulated temporal variations of methane emissions (which are mainly temperature driven) agreed well with observations. In the tropics, however, the methane model was tested against only one data set from a site which was not suitable for testing the Q_{10} of methane production, because the seasonal temperature variation was only 2^oC (and the seasonal pattern of methane emissions was mainly influenced by the seasonal pattern of the water table) [*Walter and Heimann*, 2000] Figure 11 shows simulated methane emission anomalies for the Q_{10} sensitivity test (Q_{10}=2) and the control run (Q_{10}=6) compared to observed anomalies in the atmospheric methane growth rate (as in Figure 7b of section 3.3 a simple 3-box model is used to obtain the "observed" anomalous methane source) for the HNH and the tropics, respectively. In the Q_{10} sensitivity test the amplitude of results is considerably lower than in the control run and also much lower than in the observations (Figure 11). Hence a low Q_{10} of 2 for methane production in the model does not improve the results. In the tropics (Figure 11) where in many years the model (control run) and the observations are in anti-phase, the same occurs in the Q_{10} sensitivity test, one exception being the year 1998 where the phase in the Q_{10} sensitivity test is now the same as in the observations. Therefore, the model does not seem to be overestimating

the impact of temperature versus the impact of water table on simulated methane emissions.

(3) In the tests with the 1-dimensional model a V_{max} value (maximum methane oxidation rate in oxic soil) of 20 $\mu M\ h^{-1}$ was used at most test sites, the range of used V_{max} values lying between 3 and 45 $\mu M\ h^{-1}$ [*Walter and Heimann*, 2000]. Therefore, a V_{max} value of 20 $\mu M\ h^{-1}$ is globally used in the methane model. In the V_{max} sensitivity test, global V_{max} values of 2, 10, 20 and 45 $\mu M\ h^{-1}$ are compared (Figure 12). Model runs using a larger V_{max} yield smaller methane emissions, because more methane is re-oxidized in soil. Figure 12 shows that the meridional pattern of simulated annual methane emissions does not change significantly if V_{max} is changed. However, the relative changes are bigger in higher latitudes indicating that there a larger proportion of produced methane is re-oxidized in soil than in the lower latitudes (see also Figure 2c). The patterns of interannual variations in simulated methane emission anomalies are the same for the four runs (not shown). Therefore, the choice of V_{max} cannot explain any differences in the patterns of interannual variations between simulated methane emission anomalies from wetlands and observed atmospheric methane growth rate anomalies.

(4) As shown in *Walter et al.* [this issue] in some tropical wetlands the parameterization of L leads to the unrealistic result that the annual mean water table is lower in years with higher precipitation, and vice versa. Figure 13, top, shows simulated annual methane emission anomalies from tropical wetlands compared to observed atmospheric methane growth rate anomalies for the tropics (as in Figure 7b of section 3.3 a simple 3-box model is used to obtain the "observed" anomalous methane source); Figure 13, bottom, shows relative annual temperature and precipitation anomalies for tropical wetlands. An indication that the parameterization of L has a significant effect on modeling results would be, if the difference between model results and observations in Figure 13, top, always had the opposite sign as the precipitation anomaly in Figure 13, bottom. In 6 out of 10 cases (1985, 1986, 1987, 1990, 1992, and 1993) model results would agree better with observations, if precipitation anomalies had a stronger impact on modeled methane emission anomalies; however, in the 4 remaining years the opposite is the case. Hence, there is no evidence that the parameterization of L causes differences in the patterns of interannual variations in simulated methane emission anomalies from wetlands and observed atmospheric methane growth rate anomalies. So, owing to the facts that the problem with L occurs only at some tropical wetlands (Figure 8 of *Walter et al.* [this issue]), and that it has an effect only in the dry season (Figure 7 of *Walter et al.* [this issue]) it does not seem to affect simulated methane emissions much. Although further tests with more realistic L values may be warranted.

3. 5. Interannual Variations during 1982-1993: Discussion

Figure 7 of section 3.3 and Figures 11 and 13 of section 3.4.2 compare interannual variations in simulated methane emission anomalies from wetlands with interannual variations in observed atmospheric methane growth rate anomalies. As mentioned in section 3.3, the general agreement between model results and observations is much better in the HNH than in the tropics; in the HNH a considerable part of observed atmospheric methane growth rate anomalies can be explained by methane emission anomalies from natural wetlands. However, possible contributions from other sources and/or the sinks and shortcomings in the model need to be assessed; on the modeling side the following points have been identified: (1) the parameterization of the lateral inflow, L, in the hydrologic model; (2) the use of only 1 tropical data set for testing and calibration; (3) the temperature dependency (Q_{10}) of methane production in the methane model; (4) the fact that expansion and contraction of wetland areas is not considered; (5) the omission of microtopography effects; (6) the limited number of iterations used in the global methane model; (7) errors in the input data. In the following each of these points as well as the contributions from other sources and/or the sinks will be discussed.

(1) The parameterization of the lateral inflow, L, in the hydrologic model is only problematic in some tropical wetlands. As discussed in section 3.4.2, however, it cannot contribute largely to the difference between model results and observations in the tropics.

(2) As there was only one data set covering the period of at least 1 season available from tropical wetlands, the 1-dimensional methane model could not be tested for different tropical wetlands. It is possible that at other tropical sites processes or controlling factors become important that are not included in the methane model; one example being turbulent diffusion in the standing water and its effect on transport and re-oxidation of methane. So far, it cannot be assessed how important possible other processes are and how they could change our global modeling results. Since the agreement between model results and observations was good at the tropical test site the methane model was considered to be applicable to all global wetlands.

(3) As shown in Figure 11 of section 3.4.2 using a methane production in the methane model that is less temperature dependent (i.e., a Q_{10} of 2 instead of 6) does not improve modeling results. Therefore the impact of temperature changes on simulated methane emissions is not overestimated in the model and differences between model results and observations cannot be accounted for by this.

(4) Particulary in the tropics during the transition from wet to dry season, and vice versa,

wetland areas expand and contract. This is not considered in the global methane-hydrology model, but it is expected to have an influence on seasonal and interannual methane emission patterns. In the model, it is assumed that the wetland area given by the data set of *Matthews and Fung* [1987] is the maximum area of a wetland. As discussed in *Walter et al.* [this issue] the seasonality of a wetland is introduced through the seasonality of the water table; i.e., in the model a tropical wetland dries as a whole during the dry season and the whole wetland is flooded during the wet season. A more realistic treatment of the transition between these two extreme states is necessary, but has not been possible so far. In the future we plan to use a combination of satellite data and a more complex hydrologic model that uses high resolution topographic data to derive the seasonal and interannual variation in tropical wetland areas [*Matthews et al.*, 1999].

(5) As shown in Figure 10 of section 3.4.2 considering the effect of sub-grid scale microtopography on hydrology can improve the results, particulary in the HNH. As the "micro" run was only a sensitivity test, a model to simulate the variation of the water table within a grid cell needs to be developed, in order to take the effect of microtopography more realistically into account. However, the largest differences between modeling results and observations occur in the tropics; there the differences cannot be explained by having neglected the effect of microtopography on hydrology.

(6) In the global methane model we use a standard 24 iterations to get to the equilibrium methane profile. Tests with the 1-dimensional methane model showed that if the water table changes very rapidly below the soil surface 24 iterations per day are not sufficient to acchieve equilibrium. However, this error occurs only at some East-Siberian and very few Canadian and Alaskan wetland points. There the sum of calculated methane fluxes plus total oxidation exceeds calculated production by 10-20%. As these are all regions with very low annual methane emissions (Figure 2a) this error cannot affect variations in HNH wetland emissions very much; however, it will be fixed in the future.

(7) Reanalyses comprise the best available input for an experiment like the one described in this study; however, they have errors which could cause errors in the modeling results. *Stendel and Arpe* [1997] compared ECMWF and National Center for Environmental Prediction/ National Center for Atmospheric Research (NCEP) [*Kalnay et al.*, 1996] reanalysis tropical precipitation with the Global Precipitation Climatology Centre (GPCP) precipitation data set which is a data set based on all suitable observations [*Rudolf et al.*, 1996]. They investigated 1988-1995 seasonal and interannual variations in tropical precipitation; both reanalysis data

sets differ considerably from each other and from the GPCP data set. Particulary, over Africa and north-western Argentina ECMWF reanalysis precipitation seems to be unrealistic. Furthermore, the declining trend in tropical precipitation over land (Figure 13, bottom) seems to be questionable. A simplified version of the global methane-hydrology model that calculates methane emission anomalies from natural wetlands based on precipitation and temperature anomalies [*Walter*, unpublished] shows very similar results in the HNH for the period 1982-1993, whether it is forced with ECMWF or NCEP re-analyses. In the tropics, however, the results differ considerably for the different input data. As both temperature and precipitation differ (in the HNH and the tropics), if NCEP and ECMWF reanalyses are compared, the difference in tropical precipitation is largest (not shown). These examples show that the uncertainty in the input data, particulary in tropical precipitation, is still large and can account for part of the difference between model results and observations in the tropics. As ECMWF and NCEP reanalyses have strengths and weaknesses in different regions, it might be useful to use further data sources (particulary for precipitation) to reduce these uncertainties in the future.

All significant methane sources and sinks are listed in Table 1. In principle, each of them could contribute to observed interannual variations in the atmospheric methane growth rate (the trend in the atmospheric growth rate is not discussed here). The major methane sources in the HNH are wetlands, fossil fuels, landfills, and animals; in the tropics most methane emissions come from wetlands, biomass burning, rice paddies, and animals; moreover most removal of methane by the OH sink takes place in the tropics [*Hein et al.*, 1997]. Methane emissions from animals and landfills, however, do not show large interannual variations, e.g., on order of a few Tg [*Matthews et al.*, 2000]. With the possible exception of 1992, the same seems to be valid for fossil sources [*Law and Nisbet*, 1996]; if no big changes in the FSU are assumed year-by-year changes in fossil sources are reported to be mostly positive, almost constant after 1984, and decline since the late 1980s; i.e., they show no large interannual variations. Therefore, in the HNH wetlands seem to be the only methane source showing considerable interannual variation.

Rice paddies are mostly located in the tropics. The mechanisms leading to methane emissions from rice paddies are essentially the same as in natural wetlands, although, factors controlling methane emissions are substantially altered by management practices such as fertilization and irrigation. Because the majority of methane emissions from rice paddies comes from irrigated rice paddies [*Neue and Roger*, 1993], methane emissions from this source are not expected to vary much with changes in precipitation, even though low precipitation can limit the supply of water, so that rice fields cannot be watered properly (H.-U. Neue, personal communication, 1998). However, interannual changes in temperature can have an effect on interannual variations in methane emissions from rice paddies. The temperature sensitivity of methane emissions from rice paddies seems to be smaller than in our model [*Sass et al.*, 1991; *Khalil et al.*, 1998; *van Bodegom and Stams*, 1999], however, different studies show different results [*Matthews et al.*, 1991, and references therein]. In our model experiment (using Q_{10}=6) two thirds of the interannual variations in methane emissions from tropical wetlands were explained by temperature variations (in the sensitivity test assuming Q_{10}=2 it is only one third). However, assuming an additional tropical methane source of less than 30% the size of the tropical wetland source in our model, that responds similarly to temperature cannot explain the difference between model results and observations in most years (Figure 13). As interannual changes in methane emissions from rice paddies due to changes in harvested area are small [*Matthews et al.*, 2000; *Shearer and Khalil*, 1993], too, there is not much evidence that methane emissions from rice paddies contribute largely to the observed anomalies in the atmospheric methane growth rate; however, further studies are necessary.

Biomass burning is considered a relatively small methane source of about 40 Tg yr^{-1} with a high uncertainty (Table 1). Systematic data on burned area and the amount of biomass burned in different ecosystems are still lacking [*Hao and Ward*, 1993]. Although satellite-derived information on the numbers of fires exists for some regions for the last 20 years, no quantitative relationships have been developed between number of fires, area burned, biomass oxidized, and methane emitted. Thus, it has not yet been possible to derive interannual changes in these variables. However, it seems likely that interannual variations in this methane source can be quite large because fires are controlled by climate, by anthropogenic activities, and sometimes by inadvertent spread of planned fires. Hence (part of) the discrepancy between model results and observations in the tropics could possibly be explained by interannual variations in emissions from biomass burning. Further investigations of the biomass burning source by means of, for example, remote sensing, auxiliary tracers (e.g., $\delta^{13}CH_4$, CO, or H_2) and modeling approaches are needed to quantify the contribution of this CH_4 source to the total observed interannual variation.

Bekki and Law [1997] investigated the sensitivity of the OH-sink to temperature variations from 1980-1992 employing a 2-dimensional chemistry-transport model. Variations in OH are positively correlated with temperature changes; i.e., temperature induced variations in the OH sink affect the methane growth rate in the opposite way as temperature induced variations in wetland emissions. A comparison between variations in the tropical growth rate due to OH variations (Figure 2 of [*Bekki and Law*, 1997]) and the observed variations in the tropical growth rate (Figure 11, right) shows that the patterns are quite similar (except for 1992); however, the magnitude is larger in the observations. Since most methane removal by OH takes place in the tropics [*Hein et al.*, 1997] it seems likely that interannual variations in tropical OH do have an effect on interannual variations in the tropical methane growth rate. This could also explain (part of) the discrepancy between our model results and observations in the tropics (Figure 11, right).

4. Summary and Conclusion

In this study we presented results of a global process-based, climate-sensitive methane-hydrology model to derive methane emissions from natural wetlands. The model was applied to the period from 1982-1993. We calculated total annual methane emissions from wetlands to be 260 Tg yr^{-1} which is at the high end of current estimates. Annual methane fluxes are lower in higher latitudes because of the shorter productive period, and HNH emissions constitute about 25% of the total wetland emissions. On a global and annual basis only 60% of the produced methane is emitted, the rest is re-oxidized in soil. A comparison between the meridional pattern of calculated annual methane emissions with a result from an inverse modeling study [*Hein et al.*, 1997] shows good agreement.

Our modeling results are compared to data from two wetlands in Sweden and Minnesota. At both test sites the seasonality of simulated and observed methane emissions agreed well. However, these tests demonstrate the effect of sub-grid scale variations in model parameters and input data on methane emissions. The results suggest that the parameter R_0 in the model is very high, and that different R_0 values should be used within one grid-cell to account for variations in substrate quality. In addition, sub-grid scale variations in the input data (mainly precipitation) and/or limitations in the used input data can also affect modeling results. Higher resolution data sets are needed to improve this in the future.

Simulated methane emissions show a pronounced seasonal cycle and strong interannual variations. In higher latitudes the seasonal cycle of methane emissions is controlled by the seasonal cycle of temperature; in lower latitudes the seasonal cycle of methane emissions is controlled by the seasonal cycle of the water table. Simulated methane emission anomalies were compared to observed growth rate anomalies. Our results suggest that in the HNH growth rate anomalies can, to a large extent, be explained by wetland emission anomalies; in the tropics, however, simulated methane emission anomalies do not compare well with observed growth rate anomalies. In the HNH variations in temperature and water table affect variations in methane emissions in equal parts; globally the influence of temperature variations is slightly stronger (60%). The strong negative methane emission anomaly in the HNH in 1992 is caused by a negative temperature anomaly that coincides with a negative water table anomaly. Our results suggest that reduced methane emissions from HNH wetlands contributed to the observed negative growth rate anomaly in 1992 and should be considered in future scenarios explaining this anomaly.

In the present study, the realism of the modeled interannual variability was evaluated against anomalous CH_4 source variations inferred from an inversion of the observed atmospheric CH_4 growth rates based on a simple 3-box model of atmospheric mixing. A more realistic interannual inversion of the atmospheric CH_4 records from the global observation networks [*Dlugokencky et al.*, 1998] using a comprehensive 3-dimensional atmospheric transport model would be very valuable. Although such an inversion inevitably will only determine the spatio-temporal distribution of the sum of all CH_4 sources, it would nevertheless allow a much more stringent assessment of the predictions of the wetland model.

Sensitivity tests of the global methane-hydrology model revealed that uniform temperature changes of $\pm 1\,^{\circ}C$ result in changes in methane emissions of about $\pm 20\,\%$ independent of the latitude and environmental conditions. As this global result agrees with results obtained with the 1-dimensional methane model from different wetland sites [*Walter and Heimann*, 2000] it seems to be very robust. Uniform changes in precipitation by $\pm 20\,\%$ alter simulated methane emissions by about $\pm 8\,\%$. These results indicate how large changes in methane emissions from wetlands can be under possible changed climatic conditions in the future. However, in order to assess these changes more realistically one needs to use GCM output from a global change scenario experiment as input for the methane-hydrology model.

In order to assess the role of wetland emissions in causing observed methane growth rate anomalies shortcomings in the model and possible contributions from other sources and the OH sink to observed growth rate anomalies were analyzed. Several potential problems in the model have been identified. The (1-dimensional) methane model has been tested against one tropical data set only and therefore, it is possible that processes occurring in some tropical wetlands are not included in the model. Globally a Q_{10} of 6 for methane production was used. All tests of the (1-dimensional) methane model in HNH wetlands show good agreement with data [*Walter and Heimann*, 2000], however, it is possible that a Q_{10} of 6 is too high in tropical wetlands. Expansion and contraction of wetlands due to changes in precipitation are not considered. Neglecting this change in wetland areas could therefore affect modeling results, particulary in the tropics. A "mean" water table for the whole 1^{o} by 1^{o} wetland grid-cell is used, but owing to microtopography the water table is not constant throughout the whole wetland. A sensitivity test ("micro") revealed that considering sub-grid scale variations in water table affects modeling results and sub-grid scale variations in water table need to be treated more realistically in the future. Errors in the input data are difficult to assess. Tropical precipitation seems to be the least certain input parameter, hence using additional precipitation data sources, could help reduce this problem in the future.

In the HNH the discrepancy between simulated interannual methane emission anomalies and interannual growth rate anomalies is relatively small. Our results suggest that in the HNH variations in methane emissions from wetlands contribute largely to observed methane growth rate anomalies. In the tropics, model results and observations are anti-phase most of the time. It does not seem likely that this discrepancy is caused due to the omission of an important process in the model (which cannot be excluded as the model was tested against one tropical data set only). Reducing the tropical Q_{10} did not improve the agreement between model results and observations. Including variations in tropical wetland areas and reducing the uncertainties in tropical precipitation will certainly improve our modeling results in the tropics. However, these factors are not likely to greatly change the anti-phasal behavior of model results and observations. Therefore, it seems likely that in the tropics contributions from other sources, such as biomass burning, and/or the OH sink to observed variations in the methane growth rate are stronger than in the HNH.

In order to fully explain interannual variations in atmospheric data a more comprehensive study is necessary. A 3-dimensional modeling study including climate feedbacks on wetland emissions, atmospheric chemistry and transport, and knowledge about interannual variations in anthropogenic methane sources could help clarify the results. As far as possible not only concentration measurements but also isotopic data should be used to test the results. In addition, a time-dependent inverse modeling study could further constrain proposed scenarios for interannual variations and particular anomalies.

Acknowledgments

B. Walter wants to thank Torben Christensen and Robert Clement for providing their data and for informative discussions. Thanks also to Ed Dlugokencky for discussions concerning the 1992 anomaly. The used ECMWF reanalyses were provided by the European Centre for Medium-Range Weather-Forecast in cooperation with the Deutsche Wetter Dienst (DWD).

References

Artaxo, P., F. Gerab, M.A. Yamsoe, J.V. Martins, Fine mode aerosol composition at three long-term atmospheric monitoring sites in the Amazon Basin, *J. Geophys., Res., 99*, 22,857-22,868, 1994.

Aselmann, I., P.J. Crutzen, Global distribution of natural freshwater wetlands and rice paddies, their Net Primary Productivity, seasonality and possible methane emissions, *J. Atmos. Chem.*, 8, 307-358, 1989.

Bartlett, K.B., P.M. Crill, D.I. Sebacher, R.C. Harriss, J.O. Wilson, J.M. Melack, Methane flux from the central Amazonian floodplain, *J. Geophys. Res., 93*, 1571-1582, 1988.

Bartlett, K. B., R. C. Harriss, Review and assessment of methane emissions from wetlands, *Chemosphere, 26*, 1-4, 261-320, 1993.

Bekki, S., K. S. Law, J. A. Pyle, Effects of ozone depletion on atmospheric CH_4 and CO concentrations, *Nature, 371*, 595-597, 1994.

Bekki, S., K.S. Law, Sensitivity of the atmospheric CH_4 growth rate to global temperature changes observed from 1980 to 1992, *Tellus, 49B*, 409-416, 1997.

van Bodegom, P.M., A.J.M. Stams, Effects of alternative electron acceptors and temperature on methanogenesis in rice paddy soils, *Chemosphere, 39*, 167-182, 1999.

Bogner, J.E., R.L. Sass, B.P. Walter, Model comparisons of methane oxidation across a management gradient: Wetlands, rice production systems, and landfills, *Global Biogeochem. Cycles*, in press, 2000.

Cao, M., S. Marshall, K. Gregson, Global carbon exchange and methane emission from natural wetlands: Application of a process-based model, *Journal of Geophysical Research, 101, D9*, 14399-14414, 1996.

Cao, M., K. Gregson, S. Marshall, Global methane emission from wetlands and its sensitivity to climate change, *Atmospheric Environment, 32* (19), 3293-3299, 1998.

Christensen, T.R., I.C. Prentice, J. Kaplan, A. Haxeltine, S.Sitch, Methane flux from northern wetlands and tundra, *Tellus, 48B*, 652-661, 1996.

Clement, R.J., S.B. Verma, E.S. Verry, Relating chamber measurements to eddy correlation measurements of methane flux, *J. Geophys. Res., 100* (D10), 21,047-21,056, 1995.

Conrad, R., Control of methane production in terrestrial ecosystems, in: *Exchange of trace gases between terrestrial ecosystems and the atmosphere*, ed. by M. O. Andreae and D. S. Schimel, *John Wiley & Sons*, 39-58, 1989.

Denier van der Gon, H., Changes in CH_4 emission from rice fields from 1960 to 1990s, 1. Impacts of modern rice technology, *Global Biogeochem. Cycles*, 14 (1), 61-72, 2000.

Devol, A.H., J.E. Richey, B.R. Forsberg, L.A. Martinelli, Seasonal dynamics of methane emissions from the Amazon River floodplain to the troposphere, *J. Geophys. Res., 95*, 16,417-16,426, 1990.

Dlugokencky, E. J., K. A. Masarie, P. M. Lang, P. P. Tans, Continuing decline in the growth rate of atmospheric methane, *Nature, 393, 447-450*, 1998.

Dlugokencky, E. J., K. A. Masarie, P. M. Lang, P. P. Tans, L. P. Steele, E. G. Nisbet, A dramatic decrease in the growth rate of atmospheric methane in the northern hemispere during 1992, *Geophys. Res. Lett., 21* (1), 45-48, 1994.

Dunfield P., R. Knowles, R. Dumont, T. R. Moore, Methane production and consumption in temperate and subarctic peat soils: Response to temperature and pH, *Soil Biol. Biochem., 25*, 321-326, 1993.

Dutton, E. G., J. R. Christy, Solar radiative forcing at selected locations and evidence for global lower tropospheric cooling following the eruptions of El Chichón and Pinatubo, *Geophys. Res. Lett., 19*, 2313-2316, 1992.

Etheridge, D.M., L.P. Steele, R.J. Francey, R.L. Langenfels, Atmospheric methane between 1000 A.D. and present: Evidence of anthropogenic emissions and climatic variability, *J. Geophys. Res., 103* (D13), 15,979-15,993, 1998.

Francey, R.J., M.R. Manning, C.E. Allison, S.A. Coram, D.M. Etheridge, R.L. Langenfels, D.C. Lowe, L.P. Steele, A history of $\delta^{13}C$ in atmospheric CH_4 from the Cape Grim Air Archive and Antarctic firn air, *J. Geophys. Res., 104* (D19), 23,631-23,643, 1999.

Gibson, J. K., P. Källberg, S. Uppala, A. Hernandez, A. Nomura and E. Serrano, The ECMWF Re-Analysis (ERA). 1. ERA description, *ECMWF Re-Analysis Project Report Series No. 1, European Centre for Medium-Range Weather Forecasts, Reading, U.K.*, 71 pp, 1997.

Gleason, J.F., P.K. Bhartia, J.R. Herman, R. McPeters, P. Newman, R.S. Stolarski, L. Flynn, G. Labow, D. Larko, C. Seftor, C. Wellemeyer, W.D. Komhyr, A.J. Miller, W. Planet, Record low global ozone in 1992, *Science, 260*, 523-526, 1993.

Gupta, M., S. Tyler, R. Cicerone, Modeling atmospheric $\delta^{13}CH_4$ and the causes of recent changes in atmospheric CH_4 amounts, *J. Geophys. Res., 101* (D17), 22,923-22,932, 1996.

Hansen, J., R. Ruedy, J. Glascoe, M. Sato, GISS analysis of surface temperature change, *J. Geophys. Res., 104*, D14, 30,997-31022, 1999.

Hao, W.M., D.E. Ward, Methane production from global biomass burning, *J. Geophysical Res., 98* (D11), 20,657-20,661, 1993.

Hein, R., P. J. Crutzen, M. Heimann, An inverse modeling approach to investigate the global atmospheric methane cycle, *Global Biogeochemical Cycles, 11, 1*, 43-76, 1997.

Hogan, K., R. Harriss, Comment on „A dramatic increase in the growth rate of atmospheric methane in the northern hemisphere during 1992", by E. J. Dlugokencky et al., *Geophysical Research Letters, Vol. 21*, 2445-2446, 1994.

Houweling, S., T. Kaminski, F. Dentener, J. Lelieveld, M. Heimann, Inverse modeling of methane sources and sinks using the adjoint of a global transport model, *J. Geophys. Res., 104* (D21), 26,137-26,160, 1999.

Houweling, S., Global modeling of atmospheric methane sources and sinks, dissertation, University of Utrecht, Utrecht, The Netherlands, 1999.

Kalnay, E. and 21 co-authors, The NCEP/NCAR 40-year Reanalysis Project, *Bull. Amer. Meteor. Soc.*, 77, 437-471, 1996.

Karlsdottir, S. I.S.A Isaksen, Changing methane lifetime: Possible cause for reduced growth, *Geophys. Res. Lett., 27*, 93-96, 2000.

Khalil, M.A.K., R.A. Rasmussen, Sources, sinks and seasonal cycles of atmospheric methane, *J. Geophys. Res., 88*, 5131-5144, 1983.

Khalil, M.A.K., R.A. Rasmussen, M.J. Shearer, R.W. Dalluge, L. Ren, C.-L. Duan, Factors affecting methane emissions from rice fields, *J. Geophys. Res., 103* (D19), 25,219-25,231, 1998.

Knorr, W., Satellite remote sensing and modelling of the global CO_2 exchange of land vegetation: A sythesis study, dissertation, Examensarbeit 49, Max-Planck-Inst. für Meteorol., Hamburg, Germany, 1997.

Krol, M., P.J. van Leeuwen, J. Lelieveld, Global OH trend inferred from methylchloroform measurements, *J. Geophys. Res., 103*, D9, 10697-10711, 1998.

Labitzke, K., Stratospheric temperature changes after the Pinatubo eruption, *J. Atmos. Terrest. Phys.*, 56, 1027-1034, 1994.

Law, K.S., E.G. Nisbet, Sensitivity of the CH_4 growth rate to changes in CH_4 emissions from natural gas and coal, *J. Geophys. Res., 101, D9*, 14,387-14,397, 1996.

Lelieveld, J., P. J. Crutzen, F. J. Dentener, Changing concentration, lifetime and climate forcing of atmospheric methane, *Tellus, 50B*, 128-150, 1998.

Levin, I., V. Hesshaimer, Refining of atmospheric transport model entries by the globally observed passive tracer distributions of ^{85}Krypton and Sulfur Hexafluoride (SF_6), *J. Geophys. Res., 101* (D11), 16,745-16,755, 1996.

Lowe, D. C., C. A. M. Brenninkmeijer, G. W. Brailsford, K. R. Lassey, A. J. Gomez, Concentration and ^{13}C records of atmospheric methane in New Zealand and Antarctica: evidence for changes in methane sources, *Journal of Geophysical Research, 99*, 16913-16925, 1994.

Lowe, D.C., M.R. Manning, G.W. Brailsford, A.M. Bromley, The 1991-1992 atmospheric methane anomaly: Southern hemisphere ^{13}C decrease and growth ra e fluctuations, *Geophys.*

Res. Lett., 24, 8, 857-860, 1997.

Matthews, E., I. Fung, Methane emission from natural wetlands: Global distribution, area, and environmental characteristics of sources, *Global Biogeochemical Cycles, Vol. 1, No. 1*, 1987.

Matthews, E., I. Fung, J. Learner, Methane emission from rice cultivation: Geographic and seasonal distribution of cultivated areas and emissions, *Global Biogeochem. Cycles, 5* (1), 3-24, 1991.

Matthews, E., J. E. Bogner, R. Sass, L. Augenbraun, T. Smith, Historical methane emissions from anthropogenic sources: Contributors to the declining growth rate of atmospheric methane?, *EOS, 79*, F123, 1998.

Matthews, E., C. Prigent, C. Birkett, M. Coe, Remote sensing and modeling of large-scale wetland dynamics, *EOS, 80* (46), F60, 1999.

Matthews, E., B. Walter, J. Bogner, D. Sarma, B. Portney, Understanding the role of sources in interannual variations in the growth rate of atmospheric methane concentrations for the last two decades, *EOS, 81* (19), S123, 2000.

Matthews, E., Wetlands, in *Atmospheric Methane: Its Role in the Global Environment*, edited by M. A. K. Khalil, pp. 202-233, Springer, Berlin, 2000.

Neue, H.-U., P.A. Roger, Rice agriculture: Factors controlling emissions, in *Atmospheric Methane: Sources, Sinks, and Role in Global Change*, edited by M.A.K. Khalil, pp. 254-297, Springer, Berlin, 1993.

Öquist, M.G., B.H. Svensson, Non-tidal wetlands, in: *Climate Change 1995, Impacts, Adaptations and Mitigation of Climate Change: Scientific-Technical Analysis, Contributions of Working Group II to the Second Assessment Report of the Intergovernmental Panel on Climate Change*, edited by R.T. Watson, M.C. Zinyowera, R.H. Moss, D.J. Dokken, pp. 215-239, University Press, Cambridge, 1996.

Quay, P.D., S.L. King, J. Stutsman, D.O. Wilbur, L.P. Steele, I. Fung, R.H. Gammon, T.A. Brown, G.W. Farwell, P.M. Grootes, F.H. Schmidt, Carbon isotopic composition of atmospheric CH_4: Fossil and biomass burning source strengths, *Global Biogeochem. Cycles, 5*, 1, 25-47, 1991.

Quay, P., J. Stutsman, D. Wilbur, A. Snover, E. Dlugokencky, T. Brown, The isotopic composition of atmospheric methane, *Global Biogeochem. Cycles, 13* (2), 445-461, 1999.

Reeburgh, W.S., J.Y. King, S.K. Regli, G.W. King, N.A. Auerbach, D.A. Walker, A CH_4 emission estimate for the Kuparuk River Basin, Alaska, *J. Geophys. Res., 103* (D22), 29,005-29,013, 1998.

Roulet, N.T., A. Jano, C.A. Kelly, L.F. Klinger, T.R. Moore, R. Protz, J.A. Ritter, W.R. Rouse, Role of the Hudson Bay lowland as a source of atmospheric methane, *J. Geophys. Res., 99* (D1), 1439-1454, 1994.

Rudolf, B., H. Hauschild, W. Rüth, U. Schneider, Comparison of raingauge analyses, satellite-based precipitation estimates and forecast model results, *Adv. Space. Res.*, **7**, 53-62, 1996.

Rudolph, J., Anomalous methane, *Nature, 368*, 19-20, 1994.

Sass, R.L., F.M. Fisher, F.T. Turner, M.F. Jund, Methane emission from rice fields as influenced by solar radiation, temperature, and straw incorporation, *Global Biogeochem. Cycles, 5* (4), 335-350, 1991.

Schauffler, S. M., J. S. Daniel, On the effects of stratospheric circulation changes on circulation trends, *Journal of Geophysical Research, 99*, 25747-25754, 1994.

Shearer, M.J., M.A.K. Khalil, Rice agriculture: Emissions, in *Atmospheric Methane: Sources, Sinks, and Role in Global Change*, edited by M.A.K. Khalil, pp. 230-253, Springer, Berlin, 1993.

Stendel, M., K. Arpe, Evaluation of the hydrological cycle in reanalyses and observations, Rep. 228, 52 pp., Max-Planck-Institut für Meteorologie, Hamburg, Germany, 1997.

Stieglitz, M., D. Rind, J. Famiglietti, C. Rosenzweig, An efficient approach to modeling the topographic control of surface hydrology for regional and global climate modeling, *J. Climate*, 10, 118-137, 1997.

Svensson, B.H., T.R. Christensen, E. Johansson, M. Öquist, Interdecadal variations in CO_2 and CH_4 exchange of a subarctic mire - Stordalen revisited after 20 years, *Oikos*, 85, 22-30, 1999.

Tathy, J.-P., B. Cros, R.A. Delmas, A. Marenco, J. Servant, M. Labat, Methane emission from flooded forest in Central Africa, *J. Geophys. Res.*, *97*, 6159-6168, 1992.

Tyler, S.C., D.C. Lowe, G.W. Brailsford, E. Dlugokencky, A. Manning, L.P. Steele, Carbon isotopic composition of atmospheric methane at a mid-continental site, Niwot Ridge, Colorado, *Eos Trans. AGU, 74*, 168, 1993.

Valentine, D. W., E. A. Holland, D. S. Schimel, Ecosystem and physiological controls over methane production in northern wetlands, *Journal of Geophysical Research, 99, D1*, 1563-1571, 1994.

Walter, B. P., M. Heimann, R. D. Shannon, J. R. White, A process-based model to derive methane emissions from natural wetlands, *Geophysical Research Letters, 23, 25*, 3731-3734, 1996.

Walter, B.P., Development of a process-based model to derive methane emissions from natural wetlands for climate studies, dissertation, Examensarbeit 60, Max-Planck-Inst. für Meteorol., Hamburg, Germany, 1998.

Walter, B.P., M. Heimann, A process-based, climate-sensitive model to derive methane emissions from natural wetlands: Application to five wetland sites, sensitivity to model parameters, and climate, *Global Biogeochem. Cycles*, in press, 2000.

Walter, B.P., M. Heimann, E. Matthews, Modeling modern methane emissions from natural wetlands, 1. Model Description, *J. Geophys. Res.*, this issue.

Westermann, P., Temperature regulation of methanogenesis in wetlands, *Chemosphere, 26*, 321-328, 1993.

Table 1: Methane Sources and Sinks (Tg yr^{-1})

	top-down[1]	bottom-up[2]
Sources		
animals	90 ± 20	98 ± 40
rice	69 ± 23	80 ± 50
wetlands	232 ± 27	145 ± 41
landfills	40 ± 15	48 ± 20
biomass burning	41 ± 11	40 ± 30
fossil sources[3]	103 ± 15	89 ± 45
other sources[4]		58 ± 49
total source	575	558
Sinks		
tropospheric OH	469 ± 30	485 ± 25
stratosphere	44 ± 8	40 ± 10
soil uptake	28 ± 14	30 ± 15
total sink	541	555

[1]Hein et al. [1997]

[2]Houweling et al. [1999] and references therein

[3]oil/gas production and coal mining

[4]sum of fossil fuel and domestic biofuel combustion, industrial production of iron, steel, and chemicals, termites, oceans, and volcanoes

Table 2: Sensitivity of simulated annual methane emissions to climate input

	change (%) due to "-"	change (%) due to "+"
soil temperature ±1°C	-17	+20
precipitation ±20%	-9	+8
water table ±10cm	-27	+17

Figure Captions:

Figure 1: Simulated annual mean methane fluxes (mg m^{-2} d^{-1}) (average of the 12 year simulation period 1982-1993).

Figure 2: Simulated emission and oxidation of methane. (a) Annual methane emissions per grid cell (Gg yr^{-1}); (b) annual total fractional oxidation (which is the sum of annual soil oxidation and annual rhizospheric oxidation) (%); (c) annual soil oxidation (%); and (d) annual rhizospheric oxidation (%).

Figure 3: Zonally integrated annual mean methane emissions from wetlands (Tg yr^{-1}). (a) Modeling results from this stuay; (b) results from an inverse model [*Hein et al.*, 1997]. (c) Zonally integrated wetland area distribution (10^9 m^2) from the data set of *Matthews and Fung* [1987].

Figure 4: Test of the methane model at the Stordalen mire (Sweden) (mg m^{-2} d^{-1}). Comparison between the 12 year (1982-1993) average of the mean of simulated methane emissions from the Stordalen grid-cell and its direct neighbors (± 1 standard deviation) (grey area) and observed methane emissions from minerotrophic (filled symbols) and ombrotrophic (opaque symbols) parts of the wetland for different years [*Svensson et al.*, 1999].

Figure 5: Test of the methane model at the Bog Lake peatland (Minnesota); all model results/ model input data are the mean of the Bog Lake peatland grid-cell and its direct neighbors (± 1 standard deviation) (grey areas), and all observations are depicted in black. First row, comparison between simulated and observed methane emissions (mg m^{-2} d^{-1}) from chamber and micrometeorological measurements [*Clement et al.*, 1995] for 1991 and 1992; second row, comparison between simulated water table and observed water table relative to the average hummock surface; third row, comparison between model input monthly precipitation and observed monthly precipitation for the Bog Lake peatland; forth row, comparison between model input monthly temperature and observed monthly temperature for the Bog Lake peatland.

Figure 6: Spatial-temporal variation of simulated methane emissions (Tg yr^{-1}) zonally integrated over 1° latitudinal bands.

Figure 7: Comparison between model results and observations and analysis for the whole globe (left side) and the higher northern hemisphere (HNH, >30°N) (right side). First row,

comparison between filtered simulated monthly methane emission anomalies from wetlands (black) and filtered observed monthly atmospheric growth rate anomalies (grey) (Tg yr^{-1}) (transport is considered, see text); second row, comparison between simulated annual methane emission anomalies from wetlands (black) and observed annual atmospheric growth rate anomalies (grey) (Tg yr^{-1}) (transport is considered, see text); third row, results from a factorial experiment separating the influences of temperature (grey) and water table (black) anomalies on simulated methane emission anomalies (Tg yr^{-1}); forth row, temperature (grey) and precipitation (black) anomalies (%) relative to the 1982-1993 mean, annual mean (global, left side) and May-October mean (HNH, right side). Note that y-axis units differ for global and HNH results.

Figure 8: Top, left, simulated annual methane emissions for 1992 relative to the 1982-1993 mean (%); top right, higher northern hemisphere (>30°N) May-October temperature (°C) and precipitation (%) for 1992 relative to the 1982-1993 mean; bottom left, annual precipitation (%) for 1992 relative to the 1982-1993 mean; bottom right, annual temperature (°C) for 1992 relative to the 1982-1993 mean.

Figure 9: Sensitivity tests to climate input. Comparisons of zonally integrated annual mean methane emissions from wetlands (Tg yr^{-1}) between sensitivity tests (grey) and control runs (black). (a,b) Sensitivity test of the global methane model to uniform changes in soil temperature of ±1 °; (c,d) sensitivity test of the global methane-hydrology model to uniform changes in precipitation of ±20 %; (e,f) sensitivity test of the global methane model to uniform changes in water table of ±10 cm.

Figure 10: Sensitivity test to the effect of including microtopography. Filtered simulated monthly methane emission anomalies from the "micro" run (black, see text) are compared to the control run (grey) and to the filtered observed anomalous methane growth rate (dashed) for the higher northern hemisphere (>30°N) (Tg yr^{-1}) (transport is considered, see text).

Figure 11: Sensitivity test to the temperature sensitivity (Q_{10}) of methane production. Filtered simulated monthly methane emission anomalies from the "Q_{10}=2" run (black, see text) are compared to the control run (Q_{10}=6, grey) and to the filtered observed anomalous methane growth rate (dashed) for the higher northern hemisphere (>30°N, left side) and the tropics (30°S-30°N, right side) (Tg yr^{-1}) (transport is considered, see text) .

Figure 12: Sensitivity test to the maximum methane oxidation rate, V_{max}. Zonally integrated annual mean methane emissions from wetlands (Tg yr^{-1}), for runs using different V_{max}

compared to the control run (V_{max}=20).

Figure 13: Tropical results (30°S-30°N). Top, comparison between simulated annual methane emission anomalies from wetlands (black) and observed annual methane growth rate anomalies (grey) (Tg yr^{-1}) (transport is considered, see text); bottom, annual temperature (grey) and precipitation (black) anomalies (%) relative to the 1982-1993 mean.

Figure 1

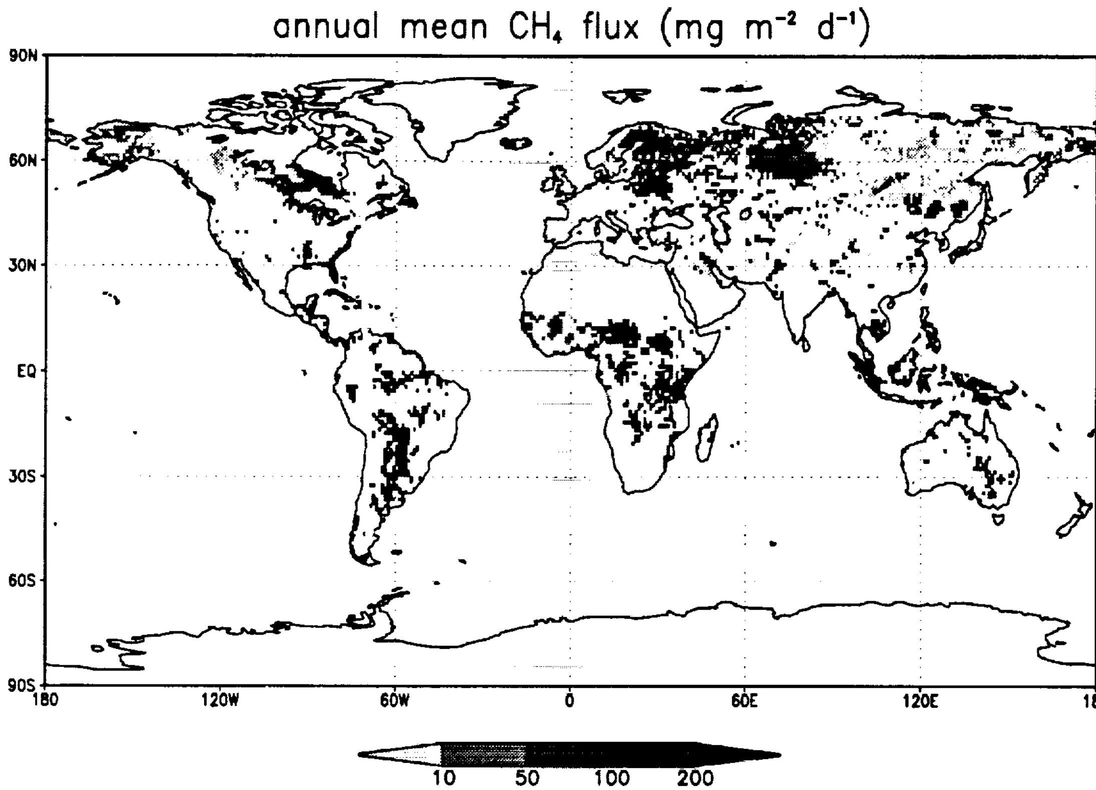
annual mean CH_4 flux (mg m^{-2} d^{-1})
90N
60N
30N
EQ
30S
60S
90S
180
120W
60W
0
60E
120E
180
10
50
100
200

Figure 2

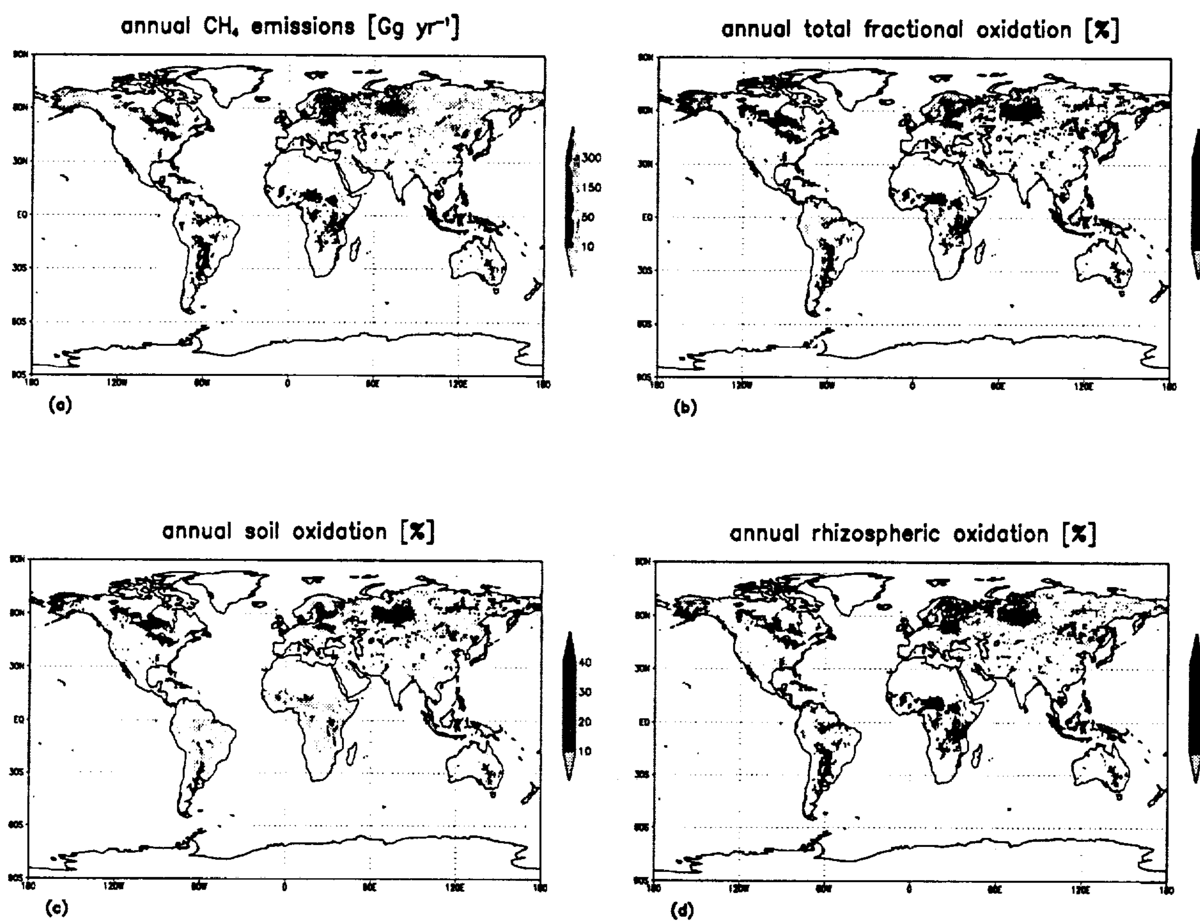
annual CH_4 emissions [Gg yr^{-1}]
300
150
50
10
(a)
annual total fractional oxidation [%]
60
50
40
30
(b)
annual soil oxidation [%]
40
30
20
10
(c)
annual rhizospheric oxidation [%]
40
30
20
10
(d)

Figure 3

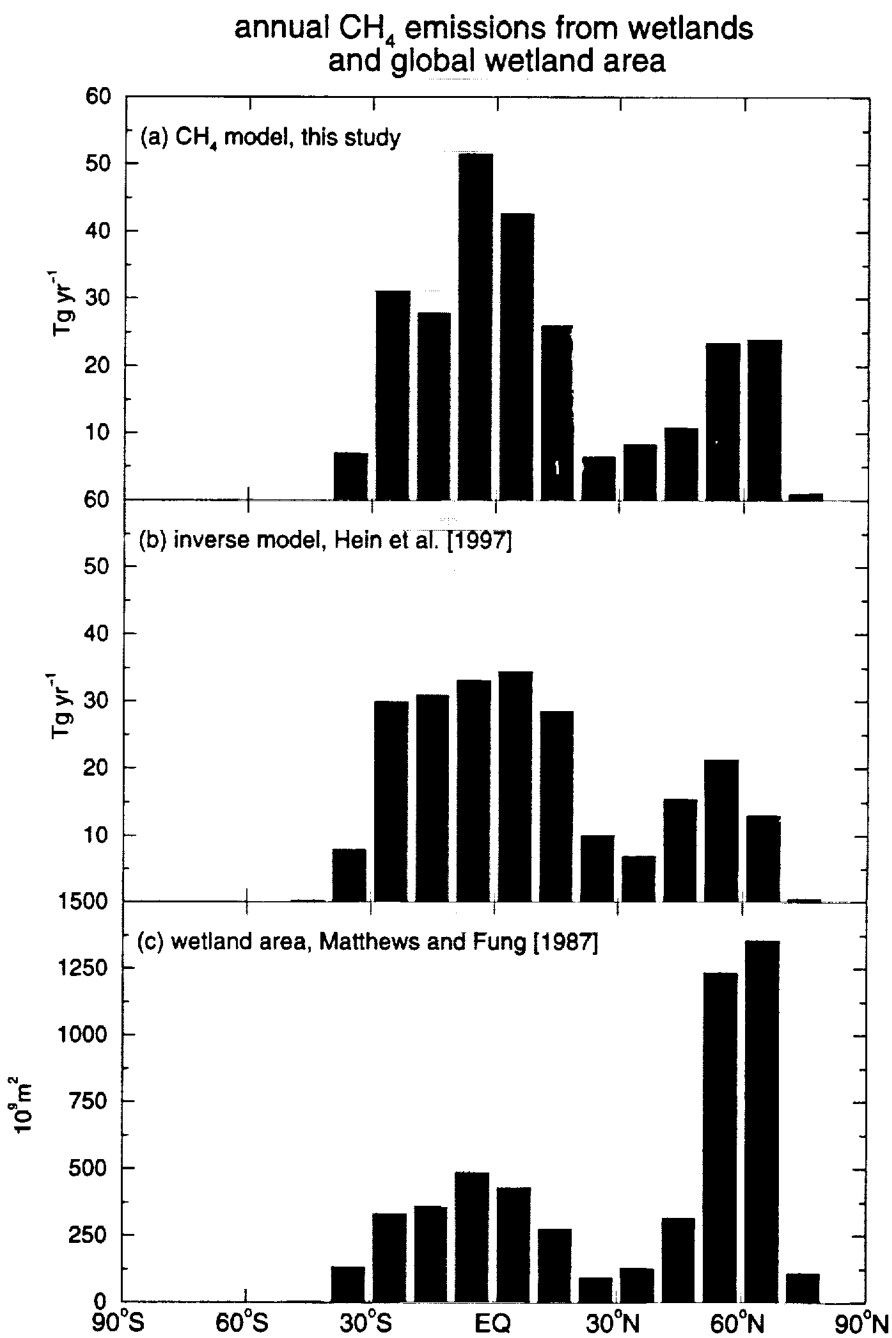

annual CH_4 emissions from wetlands
and global wetland area
(a) CH_4 model, this study
(b) inverse model, Hein et al. [1997]
(c) wetland area, Matthews and Fung [1987]
Tg yr^{-1}
Tg yr^{-1}
10^9 m^2
60
50
40
30
20
10
60
50
40
30
20
10
1500
1250
1000
750
500
250
0
90°S
60°S
30°S
EQ
30°N
60°N
90°N

Figure 4

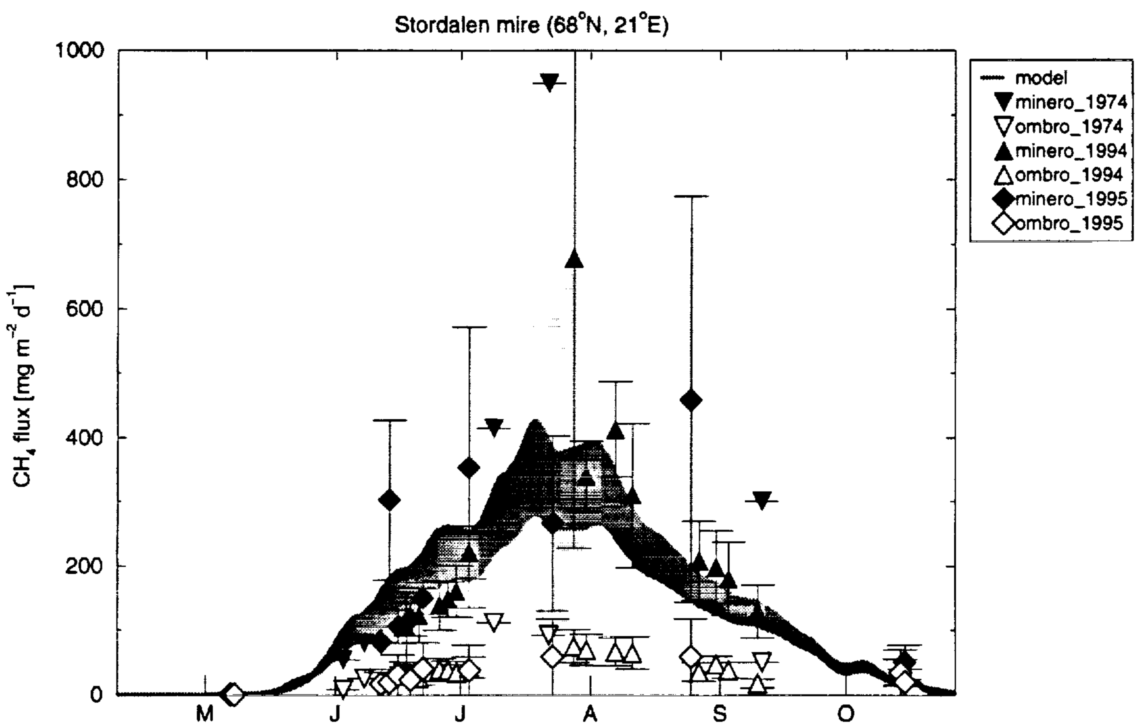

Stordalen mire (68°N, 21°E)
1000
800
600
400
200
0
CH$_4$ flux [mg m^{-2} d^{-1}]
M
J
J
A
S
O
model
minero_1974
ombro_1974
minero_1994
ombro_1994
minero_1995
ombro_1995

Figure 5

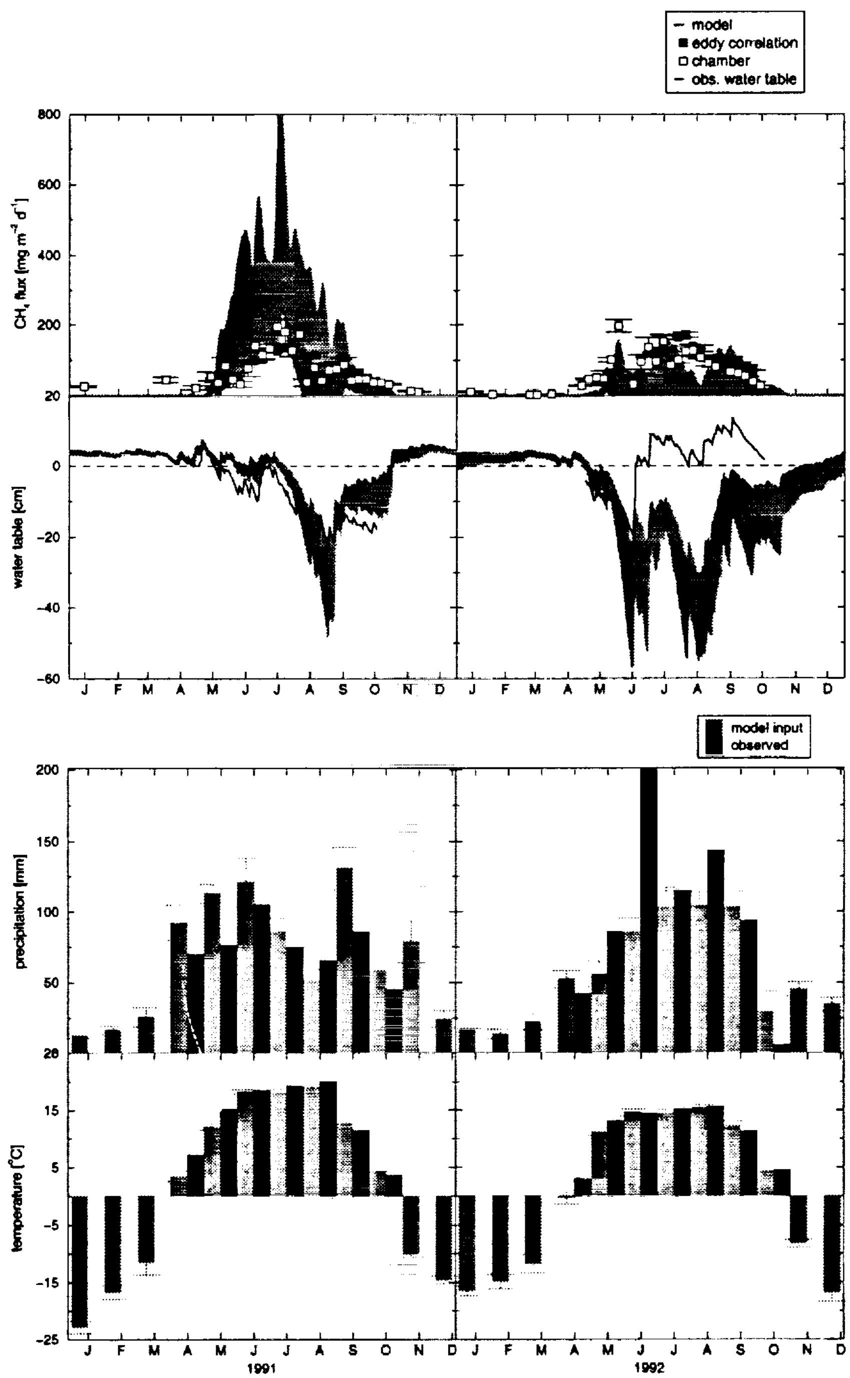

model
eddy correlation
chamber
obs. water table
CH4 flux [mg m-2 d-1]
water table [cm]
model input
observed
precipitation [mm]
temperature [°C]
J F M A M J J A S O N D
1991
1992

Figure 6

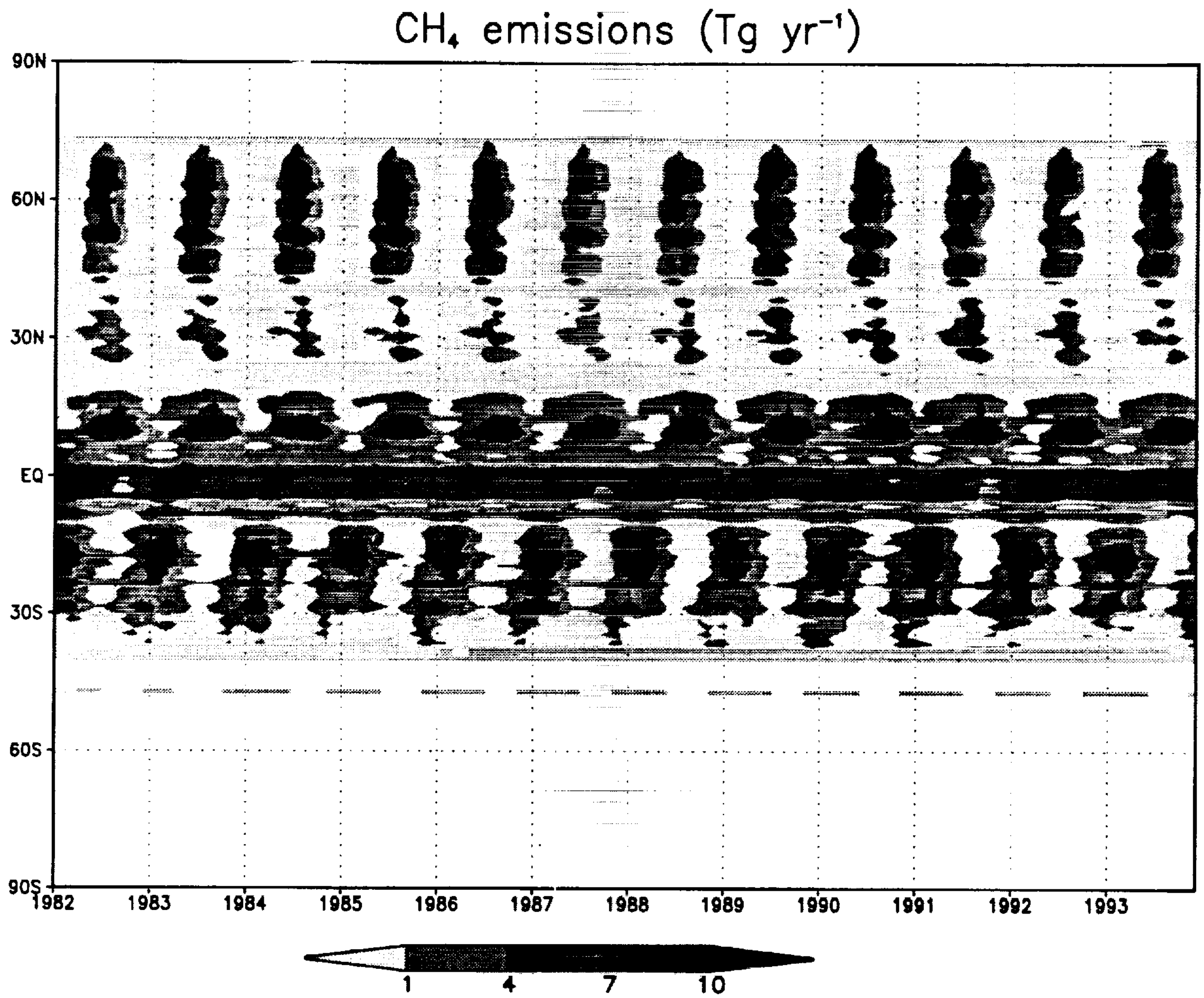
CH4 emissions (Tg yr-1)
90N
60N
30N
EQ
30S
60S
90S
1982
1983
1984
1985
1986
1987
1988
1989
1990
1991
1992
1993
1
4
7
10

Figure 7

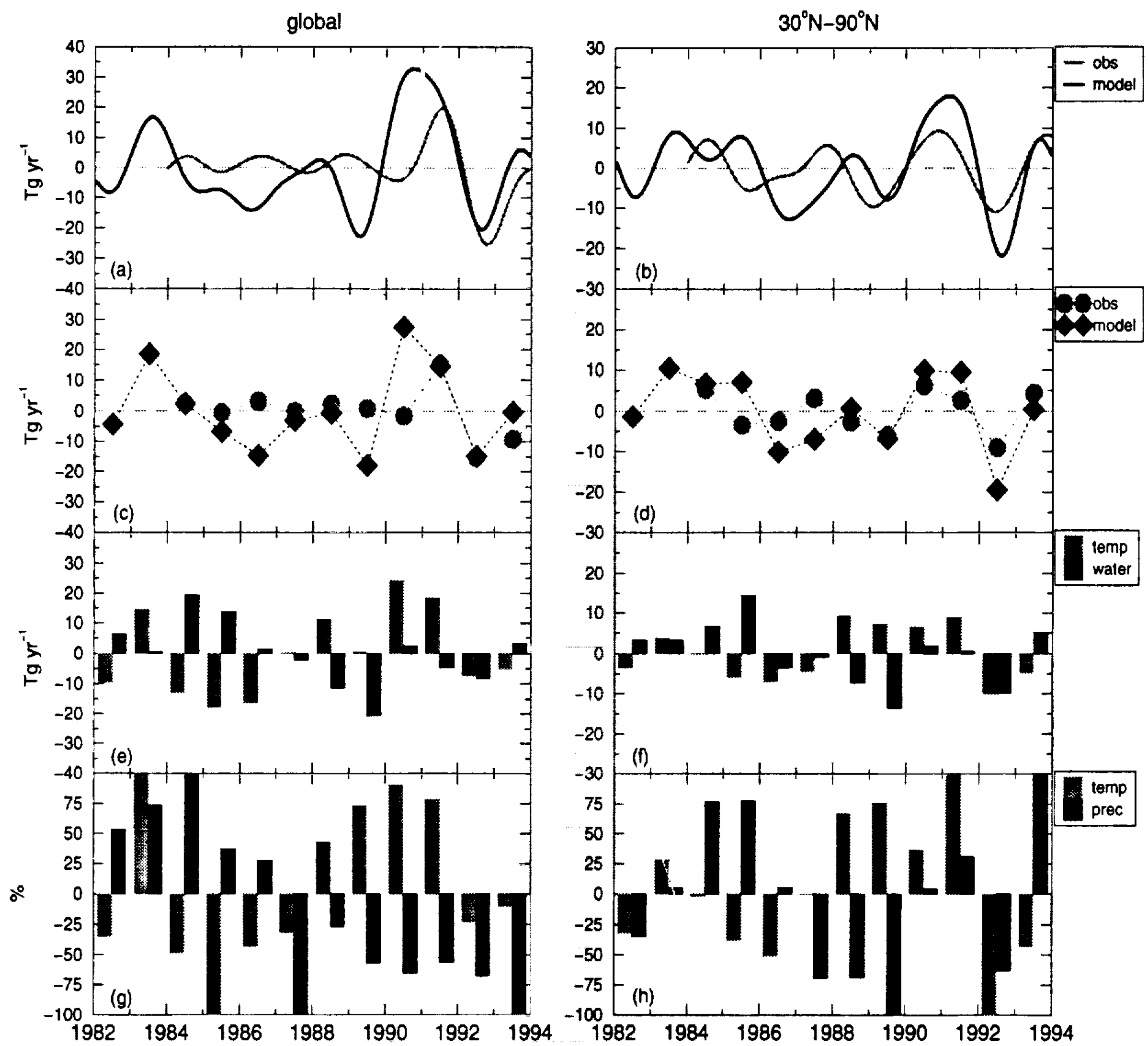

global
30°N-90°N
obs
model
temp
water
temp
prec
Tg yr⁻¹
%
(a)
(b)
(c)
(d)
(e)
(f)
(g)
(h)
1982
1984
1986
1988
1990
1992
1994

Figure 8

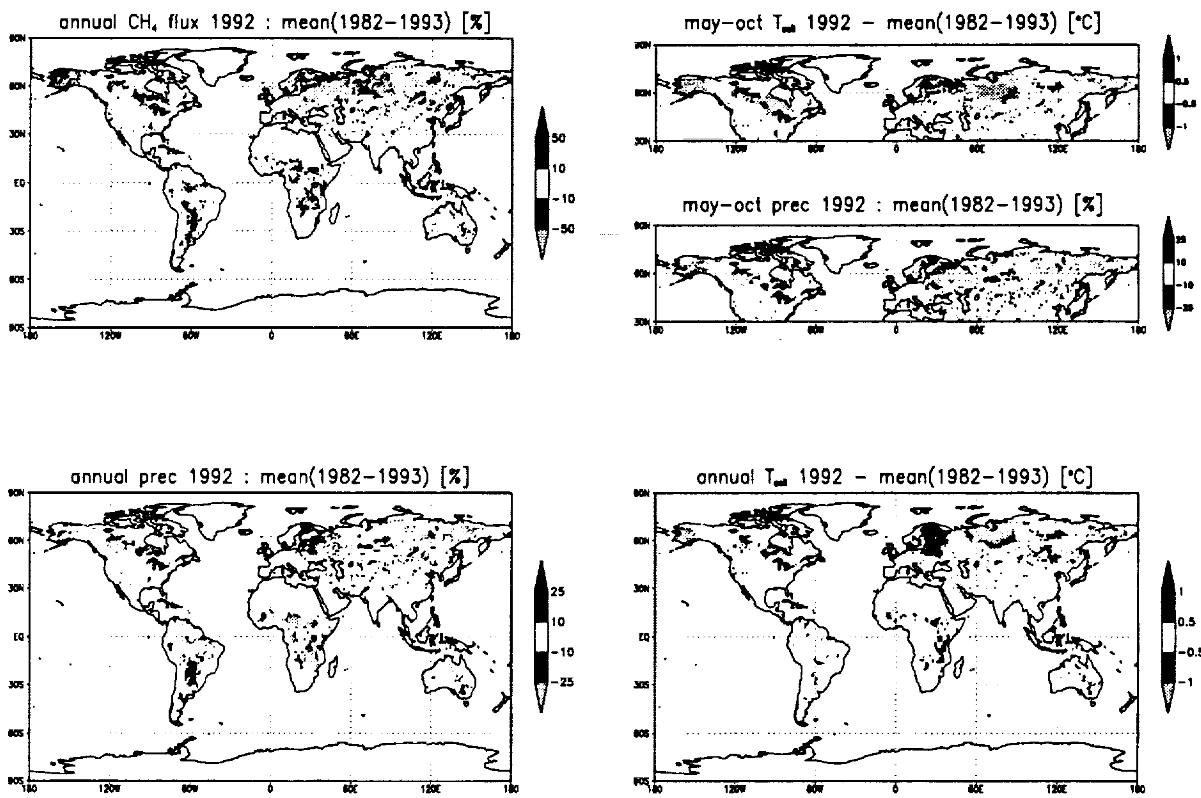
annual CH4 flux 1992 : mean(1982-1993) [%]
may-oct Tsoil 1992 - mean(1982-1993) [°C]
may-oct prec 1992 : mean(1982-1993) [%]
annual prec 1992 : mean(1982-1993) [%]
annual Tsoil 1992 - mean(1982-1993) [°C]
50
10
-10
-50
25
10
-10
-25
1
0.5
-0.5
-1
90N
60N
30N
EQ
30S
60S
90S
180
120W
60W
0
60E
120E
180

Figure 9

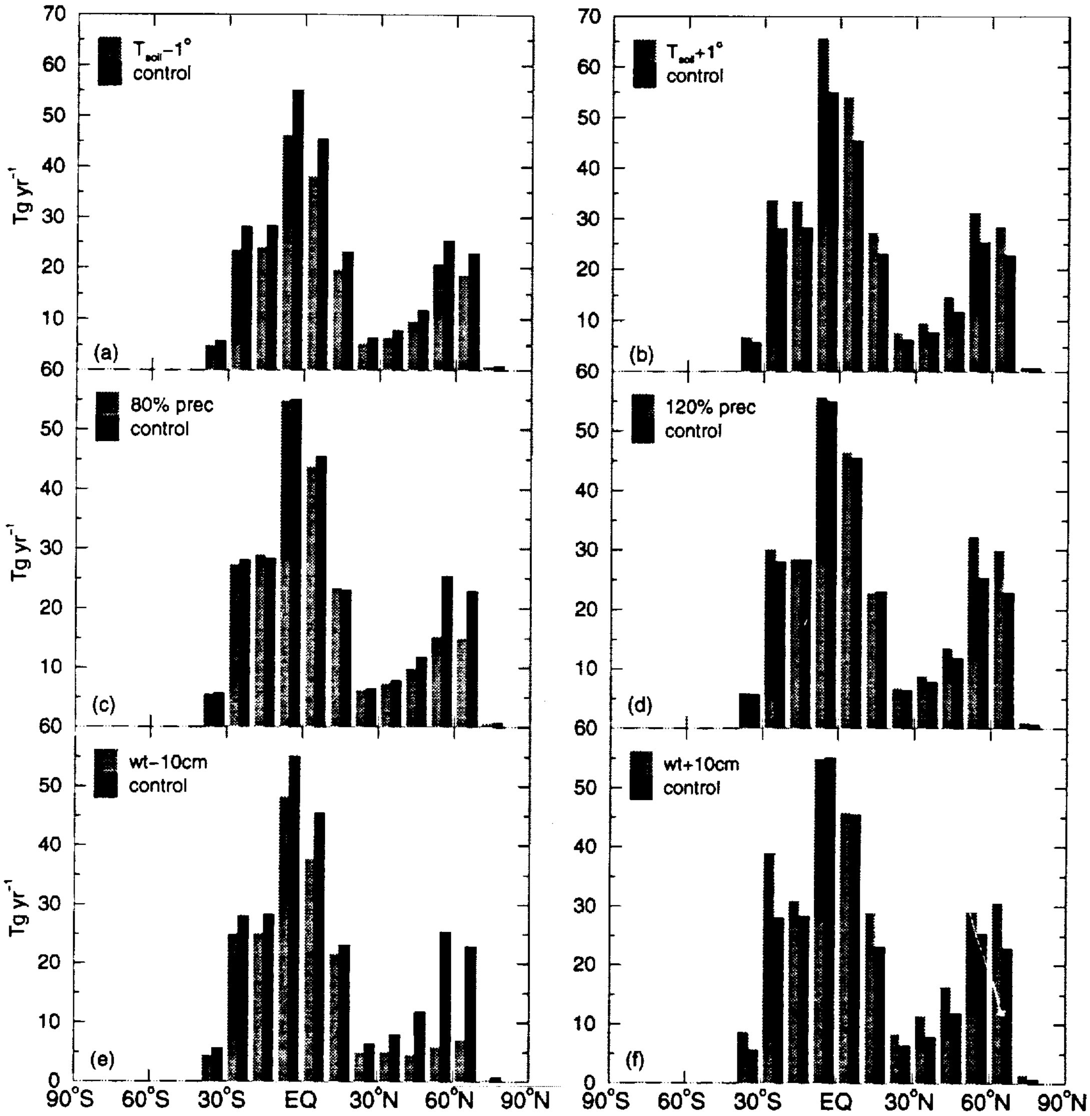

(a)
T_{soil}-1°
control
(b)
T_{soil}+1°
control
(c)
80% prec
control
(d)
120% prec
control
(e)
wt-10cm
control
(f)
wt+10cm
control
Tg yr-1
90°S 60°S 30°S EQ 30°N 60°N 90°N

Figure 10

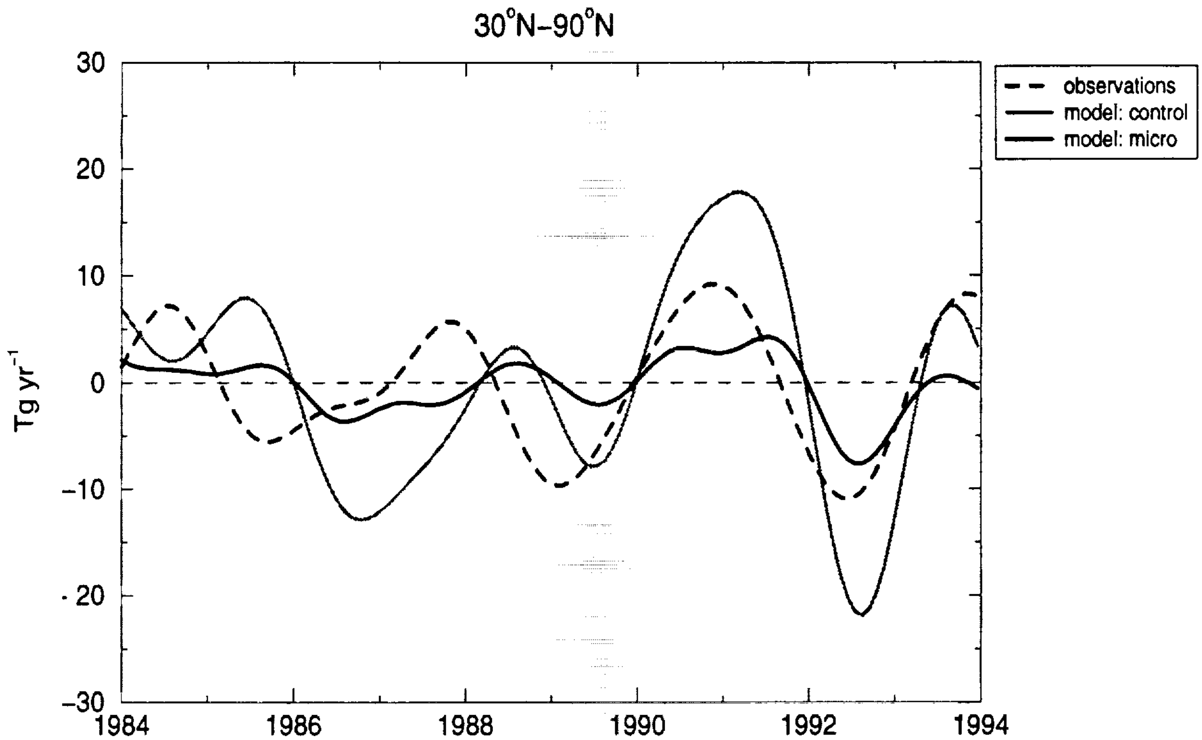
30°N-90°N
observations
model: control
model: micro
Tg yr⁻¹
30
20
10
0
-10
-20
-30
1984
1986
1988
1990
1992
1994

Figure 11

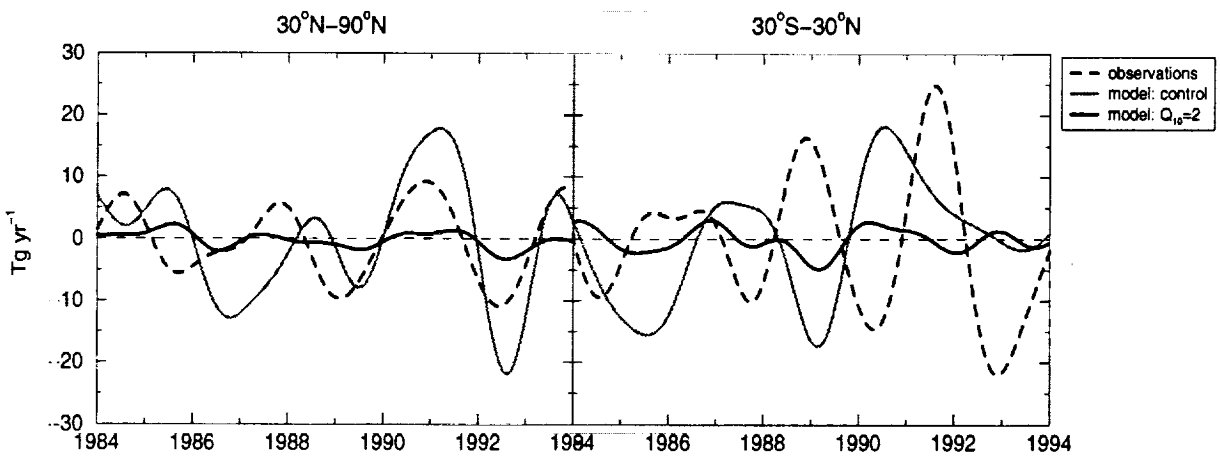
30°N-90°N
30°S-30°N
observations
model: control
model: Q10=2
Tg yr-1
30
20
10
0
-10
-20
-30
1984
1986
1988
1990
1992
1994

Figure 12

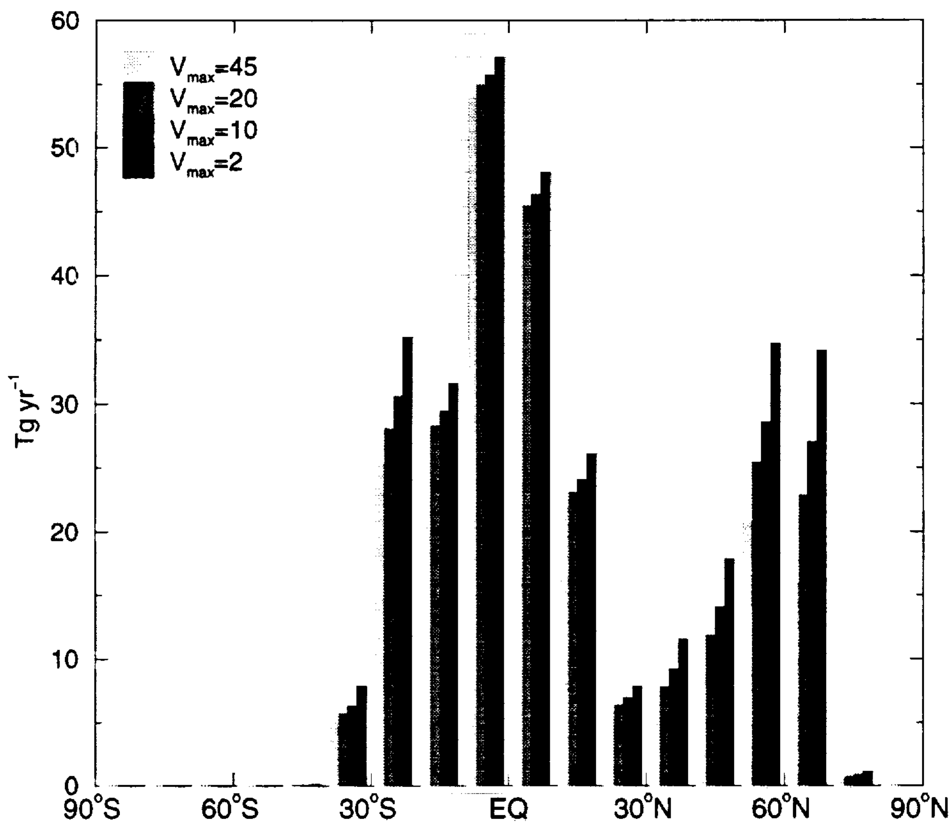

60
50
40
30
20
10
0
Tg yr⁻¹
V_{max}=45
V_{max}=20
V_{max}=10
V_{max}=2
90°S
60°S
30°S
EQ
30°N
60°N
90°N

Figure 13

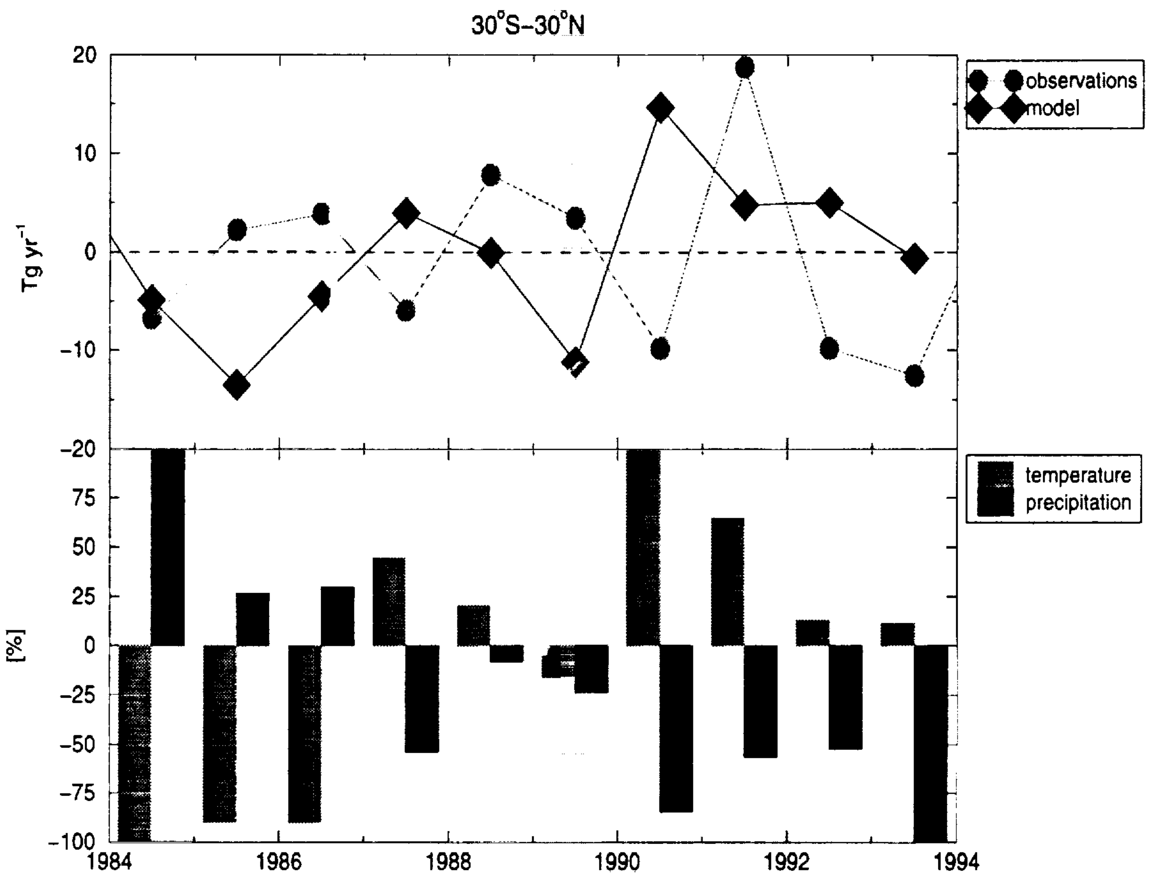

30°S–30°N
observations
model
Tg yr-1
temperature
precipitation
[%]
20
10
0
-10
-20
75
50
25
0
-25
-50
-75
-100
1984
1986
1988
1990
1992
1994